Robust Euclidean Embedding via EDM Optimization

Shenglong Zhou · Naihua Xiu · Hou-Duo Qi

Abstract This paper aims to propose an efficient numerical method for the most challenging problem known as the robust Euclidean embedding (REE) in the family of multi-dimensional scaling (MDS). The problem is notoriously known to be nonsmooth, nonconvex and its objective is non-Lipschitzian. We first explain that the semidefinite programming (SDP) relaxations and Euclidean distance matrix (EDM) approach, popular for other types of problems in the MDS family, failed to provide a viable method for this problem. We then propose a penalized REE (PREE), which can be economically majorized. We show that the majorized problem is convex provided that the penalty parameter is above certain threshold. Moreover, it has a closed-form solution, resulting in an efficient algorithm dubbed as `PREEEDM` (for Penalized REE via EDM optimization). We will prove among others that `PREEEDM` converges to a stationary point of PREE. Finally, the efficiency of `PREEEDM` will be compared with several state-of-the-art methods including SDP and EDM solvers on a large number of test problems from sensor network localization and molecular conformation.

Shenglong Zhou
School of Mathematics, University of Southampton. Southampton SO17 1BJ, UK.
E-mail: sz3g14@soton.ac.uk

Naihua Xiu
Department of Applied Mathematics, Beijing Jiaotong University, Beijing, China.
E-mail: nhxiu@bjtu.edu.cn

Hou-Duo Qi
School of Mathematics, University of Southampton, Southampton SO17 1BJ, UK.
E-mail: hdqi@soton.ac.uk

1 Introduction

This paper aims to propose an efficient numerical method for the most challenging problem in the Multi-Dimensional Scaling (MDS) family, which has found many applications in social and engineering sciences [6, 10]. The problem is known as the Robust Euclidean Embedding, a term borrowed from [8]. In the following, we first describe the problem and its three variants. We then explain our approach and our main contribution. We will postpone the relevant literature review to the next section in order to shorten the introduction part.

1.1 Problem description

The problem can be described as follows. Suppose we are given some dissimilarity measurements (e.g., noisy distances), collectively denoted as δ_{ij}, for some pairs (i, j) among n items. The problem is to find a set of n points $\mathbf{x}_i \in \Re^r$, $i = 1, \dots, n$ such that

$$d_{ij} := \|\mathbf{x}_i - \mathbf{x}_j\| \; \approx \; \delta_{ij} \quad (i, j) \in \mathcal{E}, \tag{1}$$

where $\|\mathbf{x}\|$ is the Euclidean norm (i.e., ℓ_2 norm) in $\Re^r$ and $\mathcal{E}$ is the set of the pairs (i, j), whose dissimilarities $\delta_{ij} > 0$ are known ($\mathcal{E}$ can be thought of the edge set if we treat δ_{ij} as a weighted edge distance between vertex i and vertex j, resulting in a weighted graph.) Throughout, we use ":=" or "=:" to mean "define". The space $\Re^r$ is called an embedding space and it is most interesting when r is small (e.g., $r = 2, 3$ for data visualization). One may also try to find a set of embedding points such that the squared distances approximate the squared δ_{ij}^2:

$$D_{ij} := \|\mathbf{x}_i - \mathbf{x}_j\|^2 \; \approx \; \delta_{ij}^2 \quad (i, j) \in \mathcal{E}. \tag{2}$$

A great deal of effort has been made to seek the best approximation from (1) or (2). The most robust criterion to quantify the best approximation is the **Robust Euclidean Embedding** (REE) defined by

$$\min_X \; f^{(d,1)}(\mathbf{x}_1, \dots, \mathbf{x}_n) := \sum_{i,j=1}^n W_{ij} |d_{ij} - \delta_{ij}|, \tag{3}$$

where $W_{ij} > 0$ if $\delta_{ij} > 0$ and $W_{ij} \geq 0$ otherwise (W_{ij} can be treated as a weight for the importance of δ_{ij}), and $X := [\mathbf{x}_1, \dots, \mathbf{x}_n]$ with each $\mathbf{x}_i$ being a column vector. In [1, 8], Problem (3) was referred to as a *robust variant of MDS* and is denoted as `rMDS`. We will reserve `rMDS` for the **Robust MDS** problem:

$$\min_X \; f^{(D,1)}(\mathbf{x}_1, \dots, \mathbf{x}_n) := \sum_{i,j=1}^n W_{ij} |D_{ij} - \delta_{ij}^2|. \tag{4}$$

The reference `rMDS` for the problem (4) is more appropriate because it involved the squared distances D_{ij}, which were used by the classical MDS [22, 42, 48, 52]. The preceding two problems are robust because of the robustness of the ℓ_1 norm used to quantify the errors [30, Sect. IV].

When the least squares criterion is used to (1), we have the popular model known as the Kruskal's **stress** [29] minimization:

$$\min_X \ f^{(d,2)}(\mathbf{x}_1, \ldots, \mathbf{x}_n) := \sum_{i,j=1}^n W_{ij}\Big(d_{ij} - \delta_{ij}\Big)^2, \qquad (5)$$

Similarly, when the least-squares criterion was applied to (2), we get the so-called **squared stress** [6]:

$$\min_X \ f^{(D,2)}(\mathbf{x}_1, \ldots, \mathbf{x}_n) := \sum_{i,j=1}^n W_{ij}\Big(D_{ij} - \delta_{ij}^2\Big)^2, \qquad (6)$$

In many applications such as molecular conformation [21], lower and upper bounds data on the distances can also be collected:

$$L_{ij} \leq D_{ij} \leq U_{ij}, \quad \forall \ (i,j), \qquad (7)$$

where $0 \leq L_{ij} \leq U_{ij}$. In applications such as nonlinear dimensionality reduction [46] and sensor network localization [43, 53], upper bounds U_{ij} can be computed by the shortest path distances and L_{ij} are simply set to be zero.

According to [8, Sect. 5.1], all of those problems are NP-hard. However, some problems are computationally more "difficult" to solve than the others. The most challenging one, which is also the main focus of this paper, is the problem (3) with/without the constraint (7). The difficulty comes from the nonsmooth term of ℓ_1 norm and the distance terms d_{ij} used. All other problems either involve the squared distances D_{ij} or the squared ℓ_2 norm, which make them "easier" to approximate. We will explain the reasons in the literature review part.

In contrast to all other three problems, there lacks efficient methods for the REE problem (3). One of the earliest computational papers that discuss this problem is Heiser [23], which is followed up by [28], where the Huber smoothing function was used to approximate the ℓ_1 norm near zero with a majorization technique. It was emphasized in [28] that "*the function is not differentiable at its minimum and is hard to majorize, leading to a degeneracy that makes the problem numerically unstable*". Another important method is the `PlaceCenter` (PC for short) algorithm studied in [1]. We will compare with it in the numerical part. The difficulty in solving (3) is also well illustrated by a sophisticated Semi-definite Programming (SDP) approach in [34, Sect. IV] (see the literature review part). We now describe our approach proposed in this paper.

1.2 Our approach and main contributions

Our approach heavily makes use of the concept of Euclidean Distance Matrix (EDM). We need some notation. Let $\mathcal{S}^n$ denote the space of all $n \times n$ symmetric matrices, endowed with the standard inner product. The induced norm is the Frobenius norm, denoted by $\|A\|$ for $A \in \mathcal{S}^n$. The (i,j)th element of $A \in \mathcal{S}^n$ is often written as A_{ij}. Let $\mathcal{S}_+^n$ be the cone of positive semidefinite matrices in $\mathcal{S}^n$ and we write $A \succeq 0$ for $A \in \mathcal{S}_+^n$. A matrix $D \in \mathcal{S}^n$ is called an EDM if there exists a set of points $\mathbf{x}_i \in \Re^r$, $i = 1, 2 \ldots, n$ such that the (i,j)th element of D is given by $D_{ij} := \|\mathbf{x}_i - \mathbf{x}_j\|^2$, $i, j = 1, \ldots, n$. The smallest dimension r is called the

embedding dimension of D and $r = \mathrm{rank}(JDJ)$, where $J := I - \frac{1}{n}\mathbf{1}\mathbf{1}^T$ is known as the centring matrix with I being the identity matrix in $\mathcal{S}^n$ and $\mathbf{1}$ being the vector of all ones in $\Re^n$. We use $\mathcal{D}^n$ to denote the set of all Euclidean distance matrices of size $n \times n$.

A very useful characterization for $D \in \mathcal{D}^n$ [22, 48] is

$$\mathrm{diag}(D) = 0 \qquad \text{and} \qquad -(JDJ) \succeq 0. \tag{8}$$

This result shows that $\mathcal{D}^n$ is a closed and convex cone. Moreover, a set of embedding points are generated by the classical MDS method [22, 42, 48, 52]:

$$[\mathbf{x}_1, \mathbf{x}_2, \ldots, \mathbf{x}_n] = \mathrm{diag}(\sqrt{\lambda_1}, \sqrt{\lambda_2}, \ldots, \sqrt{\lambda_r})\,[\mathbf{p}_1, \mathbf{p}_2, \ldots, \mathbf{p}_r]^T, \tag{9}$$

where the eigenvalues $\lambda_1 \geq \lambda_2 \geq \cdots \geq \lambda_r > 0$ and the corresponding eigenvectors $\mathbf{p}_1, \mathbf{p}_2, \ldots, \mathbf{p}_r$ are from the eigen-decomoposition:

$$-\frac{1}{2}(JDJ) = [\mathbf{p}_1, \mathbf{p}_2, \ldots, \mathbf{p}_r]\,\mathrm{diag}(\lambda_1, \lambda_2, \ldots, \lambda_r)\,[\mathbf{p}_1, \mathbf{p}_2, \ldots, \mathbf{p}_r]^T \tag{10}$$

with $r = \mathrm{rank}(JDJ)$. Therefore, the REE problem (3) with the constraint (7) can be reformulated in terms of EDM as

$$\begin{aligned} \min_D \; & f(D) := \sum_{i,j=1}^n W_{ij}|\sqrt{D_{ij}} - \delta_{ij}| = \|W \circ (\sqrt{D} - \Delta)\|_1 \\ \text{s.t.} \quad & D \in \mathcal{D}^n, \quad \mathrm{rank}(JDJ) \leq r \\ & D \in \mathcal{B} := \{A \mid L \leq D \leq U\}, \end{aligned} \tag{11}$$

where "$\circ$" is the Hadamard product for matrices (i.e., $A \circ B = (A_{ij}B_{ij})$), $\sqrt{D}$ is the elementwise square root of D, $\Delta_{ij} := \delta_{ij}$, and $\|\cdot\|_1$ is the ℓ_1 norm. Once we obtained an optimal solution of (11), we use (9) and (10) to generate the required embedding points.

The reformulation well captures the four difficulties in solving the REE problem (3).

(i) The objective function $f(D)$ is not convex. The term $|\sqrt{D_{ij}} - \delta_{ij}|$ is convex when $\delta_{ij}^2 > D_{ij}$ and concave otherwise.
(ii) The objective function is nonsmooth. It is not differentiable at certain points due to the ℓ_1 norm and the square root operation involved.
(iii) The objective function is not Lipschizian. The Lipschitz constant goes to infinity as D_{ij} goes to zero. The implication is that the subdifferential of the objective function [41, Def. 8.3] may be unbounded. This would create a huge obstacle in establishing any convergence results of iterative algorithms for (11).
(iv) The rank constraint is not convex and is hard to approximate. This is a common issue for any optimization problem with a rank constraint.

We note that no matter what reformulations one may use for (3), those four difficulties would appear in different forms and won't go away. We also note that all other three problems, when reformulated in terms of EDM, have a convex objective function. This distinctive feature alone makes the problem (11) the most challenging one to solve.

Existing numerical experiments have evidenced that the MDS embedding (9) and (10) works well as long as D is close to a true EDM. A typical example is when the data sits on a lower-dimensional manifold [46]. Motivated by this, we are

going to generate an approximate EDM instead of a true EDM in our algorithm. It follows from (8) that (also see [31, Thm. A]):

$$D \in \mathcal{D}^n \quad \Longleftrightarrow \quad \mathrm{diag}(D) = 0 \quad \text{and} \quad -D \in \mathcal{K}_+^n, \tag{12}$$

where $\mathcal{K}_+^n$ is known to be the conditionally positive semidefinite cone:

$$\mathcal{K}_+^n := \left\{ A \in \mathcal{S}^n \mid \mathbf{v}^T A \mathbf{v} \geq 0, \ \forall \ \mathbf{v} \in \mathbf{1}^\perp \right\}$$

and $\mathbf{1}^\perp$ is the subspace in $\Re^n$ orthogonal to $\mathbf{1}$. The diagonal constraint in (12) can be integrated to the set $\mathcal{B}$ with the choice $L_{ii} = U_{ii} = 0$ for $i = 1, \ldots, n$. We combine $\mathcal{K}_+^n$ with the rank constraint into the set $\mathcal{K}_+^n(r)$:

$$\mathcal{K}_+^n(r) := \mathcal{K}_+^n \cap \{A \in \mathcal{S}^n \mid \mathrm{rank}(JAJ) \leq r\}.$$

We call it the conditionally positive semidefinite cone with the rank-r cut. Consequently, the constraints in (11) become $-D \in \mathcal{K}_+^n(r)$ and $D \in \mathcal{B}$.

Next, we quantify the feasibility of $-D$ belonging to $\mathcal{K}_+^n(r)$ as follows. Let $\Pi_{\mathcal{K}_+^n(r)}^B(A)$ be the set of all nearest points in $\mathcal{K}_+^n(r)$ from a give matrix $A \in \mathcal{S}^n$. That is

$$\Pi_{\mathcal{K}_+^n(r)}^B(A) := \mathrm{argmin} \left\{ \|A - Y\| \mid Y \in \mathcal{K}_+^n(r) \right\}. \tag{13}$$

Since $\mathcal{K}_+^n(r)$ is not convex (unless $r >= n - 1$), the projection $\Pi_{\mathcal{K}_+^n(r)}^B(A)$ is a set instead of a single point. We let $\Pi_{\mathcal{K}_+^n(r)}(A)$ be any element in $\Pi_{\mathcal{K}_+^n(r)}^B(A)$ and define the function

$$g(A) := \frac{1}{2} \|A + \Pi_{\mathcal{K}_+^n(r)}(-A)\|^2. \tag{14}$$

Since $g(A)$ is just the half of the squared distance from $(-A)$ to $\mathcal{K}_+^n(r)$, it does not depend on which element $\Pi_{\mathcal{K}_+^n(r)}(A)$ is being used. It is easy to see that

$$-D \in \mathcal{K}_+^n(r) \qquad \text{if and only if} \qquad g(D) = 0.$$

Hence, the problem (11) is equivalent to

$$\begin{aligned} \min_D \ & f(D) = \|W \circ (\sqrt{D} - \Delta)\|_1 \\ \text{s.t.} \quad & g(D) = 0, \quad D \in \mathcal{B}. \end{aligned} \tag{15}$$

This is a classical constrained optimization problem with an equality constraint and a simple box constraint. Therefore, the quadratic penalty method [33, Chp. 17] can be applied to get the following problem:

$$\min_D \ f_\rho(D) := f(D) + \rho g(D), \qquad \text{s.t.} \ D \in \mathcal{B}, \tag{16}$$

where $\rho > 0$ is the penalty parameter. We refer to this problem as the penalized REE problem (PREE).

The quadratic penalty method is used often in practice [33, P. 497]. In fact, it is particularly suitable to (11) because it overcomes all four difficulties discussed above. We will need two more important tools to help us efficiently solve the penalty problem (16). One is the majorization technique that has recently become very popular in engineering sciences [45] (also see [6, Chp. 8] for its extensive use

in MDS). Suppose we have the current iterate D^k. We construct a majorization function $g_m(D, D^k)$ for $g(D)$ at D^k such that

$$g_m(D^k, D^k) = g(D^k) \qquad \text{and} \qquad g_m(D, D^k) \geq g(D) \quad \forall\, D \in \mathcal{S}^n. \qquad (17)$$

The majorization is constructed in such a way that it is easier to solve the majorized problem:

$$D^{k+1} = \operatorname{argmin} \left\{ f_\rho^k(D) := f(D) + \rho g_m(D, D^k), \quad D \in \mathcal{B}. \right\} \qquad (18)$$

It can be seen that

$$
\begin{aligned}
f_\rho(D^{k+1}) \;&=\; f(D^{k+1}) + \rho g(D^{k+1}) \\
&\overset{(17)}{\leq}\; f(D^{k+1}) + \rho g_m(D^{k+1}, D^k) = f_\rho^k(D^{k+1}) \\
&\overset{(18)}{\leq}\; f_\rho^k(D^k) = f(D^k) + \rho g_m(D^k, D^k) = f(D^k) + \rho g(D^k) = f_\rho(D^k).
\end{aligned}
$$

Hence, the algorithm generates a sequence $\{D^k\}$ that is nonincreasing in $f_\rho(D)$. Since $f_\rho(D)$ is bounded below by 0, the functional sequence $\{f_\rho(D^k)\}$ converges. However, we are more concerned where the iterate sequence $\{D^k\}$ converges. The second concern is how the subproblem (18) has to be solved. This brings out the second technique, which is to solve the following one-dimensional problem:

$$\min_{x \in \Re} \left\{ q(x) := (1/2)(x - \omega)^2 + \beta|\sqrt{x} - \delta| \;\mid\; a \leq x \leq b \right\}, \qquad (19)$$

for given $\delta > 0$ and $0 \leq a \leq b$. We will show that the solution of this problem will lead to a close-form solution of (18).

Since our method is for the Penalized REE by EDM optimization, we call it PREEEDM. The major contribution of this paper is to make the outlined solution procedure water-tight. In particular, we will investigate the relationship between the PREE problem (16) and the original problem (11) in terms of the ϵ-optimality (Prop. 1). We will also show that the majorization function $g_m(\cdot, \cdot)$ can be economically constructed (Subsect. 3.2). Moreover, the majorized function $f_\rho^k(D)$ is guaranteed to be convex provided that the penalty parameter is above certain threshold and the subdifferentials at the generated sequences are bounded (Prop. 4). Furthermore, each majorization subproblem has a closed form solution (Thm. 1). We are also able to prove that any accumulation of the generated sequence by PREEEDM is a stationary point of (16) (Thm. 2). Built upon its solid convergence results and simple implementation, PREEEDM is demonstrated to be comparable to six state-of-the-art software packages in terms of solution quality and outperform them in terms of the cpu for a large number of tested problems from sensor network localizations and molecular conformations.

1.3 Organization of the paper

In the next section, we give a selective literature review with the purpose that the existing approaches failed to provide a viable method for the REE problem. In Sect. 3. we introduce some necessary background and prove a key technical result

(Lemma 1) that is crucial to the convexity of the majorization subproblem. We study the relationship between the penalized REE (16) and the original REE in Sect. 4, where the majorized subproblem is shown to have a closed-form solution. In Sect. 5, we provide a complete set of convergence results for the proposed `PREEEDM` algorithm. Numerical experiments are included in Sect. 6. The paper concludes in Sect. 7.

2 Literature Review

One can find a thorough review on all of the four problems in [17] by France and Carroll, mainly from the perspective of applications. In particular, there contains a detailed and well-referenced discussion on the properties and use of the ℓ_1 and ℓ_2 norms (metrics). One can also find valuable discussion on some of those problems in [2]. So the starting point of our review is that those problems have their own reasons to be studied and we are more concerned how they can be efficiently solved.

Most of existing algorithms can be put in three groups. The first group consists of alternating coordinates descent methods, whose main variables are $\mathbf{x}_i$, $i = 1, \ldots, n$. A famous representative in this group is the method of `SMACOF` for the stress minimization (5) [13, 14]. The key idea is to alternatively minimize the function $f^{(d,2)}$ with respect to each $\mathbf{x}_i$, while keeping other points $\mathbf{x}_j$ ($j \neq i$) unchanged, and each minimization problem is relatively easier to solve by employing the technique of *majorization*. `SMACOF` has been widely used and the interested reader can refer to [6] for more references and to [53] for some critical comments on `SMACOF` when it is applied to the sensor network localization problem. The second and third group consist respectively the methods of *Semi-Definite Programming* (SDP) and *Euclidean Distance Matrix* (EDM) optimization. We will give a more detailed review on the two groups because of their close relevance to our proposed method in this paper. The main purpose of our review is to show that there lacks efficient numerical methods for the REE problem (3).

2.1 On SDP approach

We note that each of the four objective functions either involves the Euclidean distance d_{ij} or its squared $D_{ij} = d_{ij}^2$. A crucial observation is that constraints on them often have SDP relaxations. For example, it is easy to see

$$D_{ij} = d_{ij}^2 = \|\mathbf{x}_i - \mathbf{x}_j\|^2 = \|\mathbf{x}_i\|^2 + \|\mathbf{x}_j\|^2 - 2\mathbf{x}_i^T \mathbf{x}_j$$
$$= Y_{ii} + Y_{jj} - 2Y_{ij}, \tag{20}$$

where $Y := X^T X \succeq 0$. Hence, the squared distance d_{ij}^2 is a linear function of the positive semidefinite matrix Y. Consequently, the EDM cone $\mathcal{D}^n$ can be described through linear transformations of positive semidefinite matrices. One can further relax the constraint $Y = X^T X$ to $Y \succeq X^T X$. By the Schur-complement, one has

$$Z := \begin{bmatrix} Y & X^T \\ X & I_r \end{bmatrix} \succeq 0 \text{ has rank } r \iff Y = X^T X. \tag{21}$$

By dropping the rank constraint, the robust MDS problem (4) can be relaxed to a SDP, which was initiated by Biswas and Ye [15].

For the Euclidean distance d_{ij}, we introduce a new variable $T_{ij} = d_{ij}$. One may relax this constraint to $T_{ij} \leq d_{ij}$, which has a SDP representation:

$$T_{ij}^2 \leq d_{ij}^2 = D_{ij} \quad \Longleftrightarrow \quad \begin{bmatrix} 1 & T_{ij} \\ T_{ij} & D_{ij} \end{bmatrix} \succeq 0. \tag{22}$$

Combination of (20), (21) and (22) leads to a large number of SDP relaxations. Typical examples, for the robust MDS problem (4), are the SDP relaxation method [5] and the edge-based SDP relaxation method [37, 49] and [27], which leads to a comprehensive Matlab package SFSDP. For the squared stress (6), one may refer to [16, 25]. For the stress problem (5), a typical SDP relaxation can be found in [34, Problem (8)]. However, unlike the problems (4), (5) and (6), the REE problem (3) does not have a straightforward SDP relaxation. We use an attempt made in [34] to illustrate this point below.

First, it is noted that problem (3) can be written in terms of EDM:

$$\min \sum_{i,j=1}^n W_{ij} |\sqrt{D_{ij}} - \delta_{ij}|$$
$$\text{s.t.} \quad D \in \mathcal{D}^n, \quad \text{rank}(JDJ) \leq r.$$

The term $|\sqrt{D_{ij}} - \delta_{ij}|$ is convex if $\delta_{ij} > \sqrt{D_{ij}}$ and is concave otherwise. A major obstacle is how to efficiently deal with the concavity in the objective.

Secondly, by dropping the rank constraint and through certain linear approximation to the concave term, a SDP problem is proposed for (3) (see [34, Eq. (20)]):

$$\begin{aligned} \min_{D, T \in \mathcal{S}^n} \quad & \langle W, \, T \rangle \\ \text{s.t.} \quad & (\delta_{ij} - T_{ij})^2 \leq D_{ij}, \quad (i,j) \in \mathcal{E} \\ & a_{ij} D_{ij} + b_{ij} \leq T_{ij}, \quad (i,j) \in \mathcal{E} \\ & D \in \mathcal{D}^n, \end{aligned} \tag{23}$$

where the quantities a_{ij} and b_{ij} can be computed from δ_{ij}. We note that each quadratic constraint in (23) is equivalent to a positive semidefinite constraint on $\mathcal{S}_+^2$ and $D \in \mathcal{D}^n$ is a semidefinite constraint on $\mathcal{S}_+^n$ by (8). Therefore, the total number of the semidefinite constraints is $|\mathcal{E}| + 1$, resulting in a very challenging SDP even for small n. Finally, the optimal solution of (23) is then refined through a second-stage algorithm (see [34, Sect. IV(B)]). Both stages of the algorithmic scheme above would need sophisticated implementation skills and its efficiency is yet to be confirmed. The lack of efficient algorithms for (3) motivated our research in this paper.

2.2 On EDM approach

A distinguishing feature from the SDP approach is that this approach treats EDM D as the main variable, without having to rely on its SDP representation. This approach works because of the characterization (12) and that the orthogonal projection onto $\mathcal{K}_+^n$ has a closed-form formula [19, 20]. Several methods are based on this formula. The basic model for this approach is the so-called nearest EDM problem:

$$\min_{D \in \mathcal{S}^n} \quad \|D - \Delta^{(2)}\|^2 \qquad \text{s.t.} \quad \text{diag}(D) = 0 \quad \text{and} \quad -D \in \mathcal{K}_+^n, \tag{24}$$

which is a convex relaxation of (6) with the special choice $W_{ij} \equiv 1$. Here the elements of the matrix $\Delta^{(2)}$ are given by $\Delta_{ij}^{(2)} := \delta_{ij}^2$. The relaxation is obtained by dropping the rank constraint $\mathrm{rank}(JDJ) \leq r$. Since the constraints of (24) are the intersection of a subspace and a convex cone, the method of alternation projection was proposed in [19, 20] with applications to the molecule conformation [21]. A Newton's method for (24) was developed in [38]. Extensions of Newton's method for the model (24) with more constraints including general weights W_{ij}, the rank constraint $\mathrm{rank}(JDJ) \leq r$ or the box constraints (7) can be found in [3, 11, 39]. A recent application of the model (24) with a regularization term to Statistics is [54], where the problem is solved by an SDP, similar to that proposed by Toh [47].

There are two common features in this class of methods. One is that they require the objective function to be convex, which is true for the problems (4), (5) and (6) when formulated in EDM. The second feature is that the nonconvexity is only caused by the rank constraint. However, as already seen in Subsect. 1.2, the REE problem (3) in terms of EDM has a nonconvex objective coupled with the distance d_{ij} (not squared distances) being used. This has caused all existing EDM-based methods mentioned above invalid to solving (3). A latest research [55] by the authors has tried to extend the EDM approach to the stress minimization problem (5) along a similar line as outlined in Subsect. 1.2. Once again, we emphasize that the key difference between the problem (3) and (5) is about nonconvex objective vs convex objective and non-differentiability vs differentiability. Hence, the problem (3) is significantly more difficult to solve than (5). Nevertheless, we will show that it can be efficiently solved by the proposed EDM optimization.

3 Background and Technical Lemmas

In this part, we introduce the necessary background about subgradient and positive roots of a special depressed cubic equation. In particular, we will prove a technical result about a composite function between the absolute value and the square root functions. This result (Lemma 1) is in the style of Taylor-expansion for differentiable functions.

3.1 Subgradients of functions

An important function appearing in our EDM reformulation (11) of the REE problem (3) is $\phi_\delta(\cdot) : \Re_+ \mapsto \Re_+$ defined for a given constant $\delta > 0$ by

$$\phi_\delta(x) := |\sqrt{x} - \delta|, \qquad \forall \, x \geq 0,$$

where $\Re_+$ is the set of all nonnegative numbers. We will need to compute its subgradient in the sense of Rockafellar and Wets [41].

Definition 1 [41, Def. 8.3] Consider a function $f : \Re^n \mapsto \Re \cup \{-\infty, +\infty\}$ and a point $\bar{\mathbf{x}}$ with $f(\bar{\mathbf{x}})$ finite. For a vector $\mathbf{v} \in \Re^n$, one say that

(a) $\mathbf{v}$ is a *regular subgradient* of f at $\bar{\mathbf{x}}$, written $\mathbf{v} \in \widehat{\partial} f(\bar{\mathbf{x}})$, if

$$f(\mathbf{x}) \geq f(\bar{\mathbf{x}}) + \langle \mathbf{v}, \, \mathbf{x} - \bar{\mathbf{x}} \rangle + o(\|\bar{\mathbf{x}} - \mathbf{x}\|),$$

where the little 'o' term is shortened for the one-sided limit condition:

$$\liminf_{\substack{\mathbf{x}\to\bar{\mathbf{x}}\\ \mathbf{x}\neq\bar{\mathbf{x}}}} \frac{f(\mathbf{x})-f(\bar{\mathbf{x}})-\langle\mathbf{v},\ \mathbf{x}-\bar{\mathbf{x}}\rangle}{\|\mathbf{x}-\bar{\mathbf{x}}\|}\geq 0;$$

(b) $\mathbf{v}$ is a (general) *subgradient* of f at $\bar{\mathbf{x}}$, written $\mathbf{v}\in\partial f(\bar{\mathbf{x}})$, if there are sequences $\mathbf{x}^\nu\to\bar{\mathbf{x}}$ with $f(\mathbf{x}^\nu)\to f(\bar{\mathbf{x}})$ and $\mathbf{v}^\nu\in\widehat{\partial}f(\mathbf{x}^\nu)$ with $\mathbf{v}^\nu\to\mathbf{v}$.

We call $\partial f(\bar{\mathbf{x}})$ the subdifferential of f at $\bar{\mathbf{x}}$. For a given number $x\in\Re$, we define its sign by

$$\operatorname{sign}(x):=\begin{cases}\{1\} & \text{if } x>0\\ [-1,1] & \text{if } x=0\\ \{-1\} & \text{if } x<0.\end{cases}$$

Apparently, $\phi_\delta(x)$ is continuous for $x>0$ and its subdifferential at $x>0$ is given by directly applying Def. 1 (note $\delta>0$)

$$\partial\phi_\delta(x)=\frac{\operatorname{sign}(\sqrt{x}-\delta)}{2\sqrt{x}}\qquad\text{for } x>0. \tag{25}$$

We note that the subdifferential of $\phi_\delta(x)$ at $x=0$ is more complicated to describe. Fortunately, we won't need it in our analysis. We state our key lemma below.

Lemma 1 *Let $\delta>0$ be given. It holds*

$$\phi_\delta(x)-\phi_\delta(y)\leq\zeta(x-y)+\frac{(x-y)^2}{8\delta^3},\quad\forall\ x>0,\ y>0,\ \zeta\in\partial\phi_\delta(x).$$

Proof We prove it by considering three cases. Case 1: $0<x<\delta^2$; Case 2: $x>\delta^2$ and Case 3: $x=\delta^2$. For simplicity, we use $\phi(x)$ for $\phi_\delta(x)$ in our proof. Let $\zeta:=\eta/(2\sqrt{x})$, then $\zeta\in\partial\phi(x)$ is equivalent to $\eta\in\operatorname{sign}(\sqrt{x}-\delta)$.

Case 1: $0<x<\delta^2$. For this case, $\operatorname{sign}(\sqrt{x}-\delta)=\{-1\}$ and $\eta=-1$. We note that $\phi(x)=\delta-\sqrt{x}$ is convex and differentiable at $0<x<\delta^2$. Thus,

$$\phi(y)\geq\phi(x)-\frac{y-x}{2\sqrt{x}}\qquad\text{for any } 0<y<\delta^2.$$

For $y\geq\delta^2$, we have the following chain of inequalities

$$\phi(x)-\frac{y-x}{2\sqrt{x}}\leq\delta-\sqrt{x}-\frac{\delta^2-x}{2\sqrt{x}}=\delta-\left[\frac{\sqrt{x}}{2}+\frac{\delta^2}{2\sqrt{x}}\right]$$

$$\leq\delta-2\sqrt{\frac{\sqrt{x}}{2}\frac{\delta^2}{2\sqrt{x}}}=\delta-\delta=0$$

$$\leq\sqrt{y}-\delta=\phi(y),$$

Hence, we proved the conclusion for this case.

Case 2: $x>\delta^2$. For this case, $\operatorname{sign}(\sqrt{x}-\delta)=\{1\}$ and $\eta=1$. By defining $\Phi(\theta,\mu):=\theta(\theta^2-\mu^2)^2-4\delta^3(\theta+\mu)^2+16\theta\delta^4$ with $\theta>\delta$ and $0<\mu<\delta$, we have

$$\frac{\partial\Phi(\theta,\mu)}{\partial\mu}=2(\theta+\mu)(2\theta\mu(\mu-\theta)-4\delta^3)\leq 0,$$

which indicates $\Phi(\theta, \mu)$ is non-increasing with respect μ and thus

$$
\begin{aligned}
\Phi(\theta, \mu) \geq \Phi(\theta, \delta) &= \theta(\theta^2 - \delta^2)^2 - 4\delta^3(\theta + \delta)^2 + 16\delta^4\theta \\
&= (\theta + \delta)^2(\theta(\theta - \delta)^2 - 4\delta^3) + 16\delta^4\theta \\
&\geq (\delta + \delta)^2(\delta(\delta - \delta)^2 - 4\delta^3) + 16\delta^5 \\
&= 0.
\end{aligned}
\tag{26}
$$

For $0 < y < \delta^2$, we have

$$
\begin{aligned}
\phi(x) - \phi(y) \;=\; & \sqrt{x} + \sqrt{y} - 2\delta = \frac{x - y}{2\sqrt{x}} + \frac{(\sqrt{x} + \sqrt{y})^2}{2\sqrt{x}} - 2\delta \\
=\; & \frac{x - y}{2\sqrt{x}} + \frac{(x - y)^2}{8\delta^3} - \left[\frac{(x - y)^2}{8\delta^3} - \frac{(\sqrt{x} + \sqrt{y})^2}{2\sqrt{x}} + 2\delta \right] \\
=\; & \frac{x - y}{2\sqrt{x}} + \frac{(x - y)^2}{8\delta^3} - \frac{\Phi(\sqrt{x}, \sqrt{y})}{8\delta^3\sqrt{x}} \\
\overset{(26)}{\leq}\; & \frac{x - y}{2\sqrt{x}} + \frac{(x - y)^2}{8\delta^3}
\end{aligned}
$$

For $y \geq \delta^2$, we have the following chain of inequalities

$$
\begin{aligned}
\phi(x) - \phi(y) &= \sqrt{x} - \sqrt{y} = \frac{x - y}{2\sqrt{x}} + \frac{(\sqrt{x} - \sqrt{y})^2}{2\sqrt{x}} \\
&= \frac{x - y}{2\sqrt{x}} + \frac{(x - y)^2}{2\sqrt{x}(\sqrt{x} + \sqrt{y})^2} \\
&\leq \frac{x - y}{2\sqrt{x}} + \frac{(x - y)^2}{2\delta(\delta + \delta)^2} \\
&= \frac{x - y}{2\sqrt{x}} + \frac{(x - y)^2}{8\delta^3}.
\end{aligned}
\tag{27}
$$

Hence, we proved the claim for this case.

Case 3: $x = \delta^2$. For this case, $\mathrm{sign}(\sqrt{x} - \delta) = [-1, 1]$ and $-1 \leq \eta \leq 1$. For $0 < y < \delta^2$, we have

$$
\begin{aligned}
\phi(x) - \phi(y) &= \delta - \sqrt{x} - (\delta - \sqrt{y}) \\
&= \sqrt{y} - \sqrt{x} = \frac{y - x}{\sqrt{y} + \sqrt{x}} \leq -\frac{x - y}{2\sqrt{x}} \leq \frac{\eta(x - y)}{2\sqrt{x}}.
\end{aligned}
$$

where the first and last inequalities hold due to $y < \delta^2 = x$ and $|\eta| \leq 1$. For $y \geq \delta^2$, similar to obtaining (27), we have

$$
\phi(x) - \phi(y) = \sqrt{x} - \sqrt{y} \leq \frac{x - y}{2\sqrt{x}} + \frac{(x - y)^2}{8\delta^3} \leq \frac{\eta(x - y)}{2\sqrt{x}} + \frac{(x - y)^2}{8\delta^3},
$$

where the last inequality is due to $|\eta| \leq 1$ and $x - y \leq 0$

For all three cases, we proved our claim and hence accomplish our proof.   □

3.2 Construction of the majorization function

A major building block in our algorithm is the majorization function $g_m(D, D^k)$ at a given point D^k for the function $g(A)$ defined in (14). We construct it below.

Suppose $A \in \mathcal{S}^n$ has the following eigenvalue-eigenvector decomposition:

$$A = \lambda_1 \mathbf{p}_1 \mathbf{p}_1^T + \lambda_2 \mathbf{p}_2 \mathbf{p}_2^T + \cdots + \lambda_n \mathbf{p}_n \mathbf{p}_n^T, \tag{28}$$

where $\lambda_1 \geq \lambda_2 \geq \ldots \geq \lambda_n$ are the eigenvalues of A in non-increasing order, and $\mathbf{p}_i$, $i = 1, \ldots, n$ are the corresponding orthonormal eigenvectors. We define a PCA-style matrix truncated at r:

$$\mathrm{PCA}_r^+(A) := \sum_{i=1}^r \max\{0, \lambda_i\} \mathbf{p}_i \mathbf{p}_i^T. \tag{29}$$

Recall the definition of $\Pi_{\mathcal{K}_+^n(r)}^B(A)$ in (13). We let $\Pi_{\mathcal{K}_+^n(r)}(A)$ be (any) one element in $\Pi_{\mathcal{K}_+^n(r)}^B(A)$ and note that the function $g(A)$ in (14) does not depend on the choice of $\Pi_{\mathcal{K}_+^n(r)}(A)$. As seen from the known results below, one particular element $\Pi_{\mathcal{K}_+^n(r)}(A)$ can be computed through $\mathrm{PCA}_r^+(A)$.

Lemma 2 *For a given matrix $A \in \mathcal{S}^n$ and an integer $r \leq n$. The following results hold.*

(i) *[39, Eq. (22), Prop. 3.3] One particular $\Pi_{\mathcal{K}_+^n(r)}(A)$ can be computed through*

$$\Pi_{\mathcal{K}_+^n(r)}(A) = \mathrm{PCA}_r^+(JAJ) + (A - JAJ) \tag{30}$$

(ii) *[39, Eq. (26), Prop. 3.3] We have*

$$\langle \Pi_{\mathcal{K}_+^n(r)}(A), \ A - \Pi_{\mathcal{K}_+^n(r)}(A) \rangle = 0. \tag{31}$$

(iii) *[39, Prop. 3.4] The function*

$$h(A) := \frac{1}{2} \| \Pi_{\mathcal{K}_+^n(r)}(A) \|^2$$

is well defined and is convex. Moreover,

$$\Pi_{\mathcal{K}_+^n(r)}(A) \in \partial h(A),$$

where $\partial h(A)$ is the subdifferential of $h(\cdot)$ at A.

(iv) *[55, Lemma 2.2] Let $g(A)$ be defined in (14). We have for any $A \in \mathcal{S}^n$*

$$g(A) = \frac{1}{2} \|A\|^2 - h(-A) \quad and \quad \| \Pi_{\mathcal{K}_+^n(r)}(A) \| \leq 2 \|A\|. \tag{32}$$

Since $h(\cdot)$ is convex and $\Pi_{\mathcal{K}_+^n(r)}(A) \in \partial h(A)$ (Lemma 2)(ii)), we have

$$h(-D) \geq h(-Z) + \langle \Pi_{\mathcal{K}_+^n(r)}(-Z), \ -D + Z \rangle \qquad \forall \, D, Z \in \mathcal{S}^n.$$

This, with Lemma 2(iii), implies

$$
\begin{aligned}
g(D) &= (1/2)\|D\|^2 - h(-D) \\
&\leq (1/2)\|D\|^2 - h(-Z) + \langle \Pi_{\mathcal{K}_+^n(r)}(-Z),\ D - Z \rangle \\
&= (1/2)\|D + \Pi_{\mathcal{K}_+^n(r)}(-Z)\|^2 + \langle \Pi_{\mathcal{K}_+^n(r)}(-Z),\ -Z - \Pi_{\mathcal{K}_+^n(r)}(-Z) \rangle \\
&\overset{(31)}{=} (1/2)\|D + \Pi_{\mathcal{K}_+^n(r)}(-Z)\|^2 \\
&=: g_m(D, Z).
\end{aligned}
\tag{33}
$$

It is straightforward to check that the function $g_m(\cdot, \cdot)$ in (33) satisfies the majorization properties (17).

3.3 Positive roots of depressed cubic equations

In our algorithm, we will encounter the positive root of a depressed cubic equation [7, Chp. 7], which arises from the optimality condition of the following problem

$$
\min_{x \geq 0} \quad s(x) := (x - t)^2 + \nu \sqrt{x},
\tag{34}
$$

where $\nu > 0$ and $t \in \Re$ are given. A positive stationary point x must satisfy the optimality condition

$$
0 = s'(x) = 2(x - t) + \frac{\nu}{2\sqrt{x}}.
\tag{35}
$$

Let $y := \sqrt{x}$. The optimality condition above becomes

$$
4y^3 - 4ty + \nu = 0.
$$

This is in the classical form of the so-called depressed cubic equation [7, Chp. 7]. Its roots (complex or real) and their computational formulae have a long history with fascinating and entertaining stories. A comprehensive revisit of this subject can be found in Xing [50] and a successful application of the depressed cubic equation to the compressed sensing can be found in [35,51]. The following lemma says that, under certain conditions, the equation (35) has two distinctive positive roots and its proof is a specialization of [9, Lem. 2.1(iii)] when $p = 1/2$ therein.

Lemma 3 *[9, Lemma 2.1(iii)] Consider the problem (34). Let*

$$
\bar{x} = (\nu/8)^{2/3} \qquad and \qquad \bar{t} = 3\bar{x}.
$$

When $t > \bar{t}$, $s(x)$ has two different positive stationary point $\hat{x}_1$ and $\hat{x}_2$ satisfying

$$
s'(x) = 0 \qquad and \qquad \hat{x}_1 < \bar{x} < \hat{x}_2.
$$

4 Penalized REE Model and Its' Majorization Subproblem

With the preparation above, we are ready to address our penalized REE problem (16) and its majorization subproblem (18). We first address the relationship between (16) and its original problem (11). We then show how the subproblem (18) is solved.

4.1 ϵ-optimal solution

The classical results on penalty methods in [33] on the differentiable case (i.e., all functions involved are differentiable) are not applicable here. Recently, the penalty approach was studied by Gao in her PhD thesis [18] in the context of semidefinite programming, which motivated our investigation below. The main result is that (16) provides an ϵ-optimal solution for the original problem when the penalty parameter is above certain threshold.

Definition 2 (ϵ-optimal solution) Suppose D^* is an optimal solution of (11). For a given error tolerance $\epsilon > 0$, a point $\widehat{D}$ is called an ϵ-optimal solution of (11) if it satisfies

$$\widehat{D} \in \mathcal{B}, \quad g(\widehat{D}) \leq \epsilon \quad \text{and} \quad f(\widehat{D}) \leq f(D^*).$$

Obviously, if $\epsilon = 0$, $\widehat{D}$ would be an optimal solution of (11). We will show that the optimal solution of (16) is ϵ-optimal provided that ρ is large enough. Let D_ρ^* be an optimal solution of the penalized REE (16) and D_r be any feasible solution of the original problem (11). If the lower bound matrix $L \equiv 0$, then we can simply choose $D_r = 0$. Define

$$\rho_\epsilon := f(D_r)/\epsilon.$$

We have the following result.

Proposition 1 *For any $\rho \geq \rho_\epsilon$, D_ρ^* must be ϵ-optimal. That is,*

$$D_\rho^* \in \mathcal{B}, \qquad g(D_\rho^*) \leq \epsilon \qquad and \qquad f(D_\rho^*) \leq f(D^*).$$

Proof Since D_ρ^* is an optimal solution of (16), we have $D_\rho^* \in \mathcal{B}$. For any feasible solution D to (11) (i.e., $g(D) = 0, D \in \mathcal{B}$ in (15)), it holds the following chain of inequalities.

$$\begin{aligned}
f(D) &= f(D) + \rho g(D) && \text{(because } g(D) = 0) \\
&= f_\rho(D) \\
&\geq f_\rho(D_\rho^*) && \text{(because } D_\rho^* \text{ minimizes (16))} \\
&= f(D_\rho^*) + \rho g(D_\rho^*) \\
&\geq \max\{f(D_\rho^*), \rho g(D_\rho^*)\}, && \text{(because } \rho, f, g \geq 0)
\end{aligned}$$

which together with the feasibility of D_r to (11) yields

$$g(D_\rho^*) \leq \frac{f(D_r)}{\rho} \leq \frac{f(D_r)}{\rho_\epsilon} = \epsilon$$

and the feasibility of D^* to (11) derives

$$f(D^*) \geq f(D_\rho^*).$$

This completes our proof. $\square$

4.2 Solving the Subproblem

Having constructed the majorization function in (33), we now focus on how to solve the majorization subproblem (18), which is equivalent to the solution of the following problem. Given the current iterate $Z \in \mathcal{B}$, the majorization subproblem aims to compute an improved iterate, denoted by Z^+, by solving

$$
\begin{aligned}
Z^+ &= \arg\min_{D \in \mathcal{B}} \; f(D) + \rho g_m(D, Z) \\
&= \arg\min_{D \in \mathcal{B}} \sum_{i,j=1}^{n} W_{ij} |\sqrt{D_{ij}} - \delta_{ij}| + \frac{\rho}{2} \| D + \Pi_{\mathcal{K}_+^n(r)}(-Z) \|^2 \\
&= \arg\min_{D \in \mathcal{B}} \sum_{i,j=1}^{n} W_{ij} |\sqrt{D_{ij}} - \delta_{ij}| + \frac{\rho}{2} \| D - Z_K \|^2,
\end{aligned}
\tag{36}
$$

where the matrix $Z_K := -\Pi_{\mathcal{K}_+^n(r)}(-Z)$. This subproblem has a perfect separability property that allows it to be computed elementwise:

$$
\begin{aligned}
Z_{ij}^+ &= \arg\min_{L_{ij} \leq D_{ij} \leq U_{ij}} \frac{\rho}{2} \left[D_{ij} - (Z_K)_{ij} \right]^2 + W_{ij} |\sqrt{D_{ij}} - \delta_{ij}| \\
&= \arg\min_{L_{ij} \leq D_{ij} \leq U_{ij}} \frac{1}{2} \left[D_{ij} - (Z_K)_{ij} \right]^2 + \frac{W_{ij}}{\rho} |\sqrt{D_{ij}} - \delta_{ij}|.
\end{aligned}
\tag{37}
$$

For the ease of our description, we denote the subproblem solution process by

$$
Z^+ = \texttt{PREEEDM}_{\mathcal{B}}(Z_K, \, W/\rho, \, \Delta).
\tag{38}
$$

Here, $\texttt{PREEEDM}$ stands for the Penalized REE by EDM optimization. We will show how $\texttt{PREEEDM}$ can be computed.

Let us consider a simplified one-dimensional optimization problem, whose solution will eventually give rise to $\texttt{PREEEDM}$. Let B denote the interval $[a, b]$ in $\Re$ with $0 \leq a \leq b$. For given $\omega \in \Re, \delta > 0$ and $\beta > 0$, we aim to compute

$$
\texttt{dcroot}_B[\omega, \beta, \delta] := \arg\min_{a \leq x \leq b} \; q(x) := \frac{1}{2}(x - \omega)^2 + \beta|\sqrt{x} - \delta|.
\tag{39}
$$

The acronym $\texttt{dcroot}$ stands for the root of depressed cubic equation, which will eventually give rise to the solution formula of (39). It suffices to consider the case that matters to us:

$$
\beta > 0, \quad \delta > 0 \quad \text{and} \quad a \leq \delta^2 \leq b.
$$

Before solving the above problem, we define some notation for convenience

$$
\begin{cases}
\gamma_{\omega,\beta} := \dfrac{\left[\omega + \sqrt{\omega^2 + 2\beta} \right]^2}{4}, & u := \dfrac{\beta}{4}, \quad v := \dfrac{\omega}{3} \quad \text{and} \quad \tau := u^2 - v^3 \\
B_- := [a, \, \delta^2] \qquad \text{and} \qquad B_+ := [\delta^2, \, b].
\end{cases}
\tag{40}
$$

Obviously, $q(x)$ has a representation of two pieces:

$$
q(x) = \begin{cases}
q_-(x) := \frac{1}{2}(x - \omega)^2 - \beta\sqrt{x} + \beta\delta & \text{for } x \in B_- \\
q_+(x) := \frac{1}{2}(x - \omega)^2 + \beta\sqrt{x} - \beta\delta & \text{for } x \in B_+
\end{cases}
$$

It is noted that $q_-(x)$ is convex, but $q_+(x)$ may not necessarily so. We will show that both pieces have a closed-form formula for their respective minimum.

Proposition 2 *Consider the optimization problem:*

$$x_-^* := \arg\min q_-(x), \qquad s.t. \;\; x \in B_-. \tag{41}$$

Define

$$x_{\omega,\beta}^- = \begin{cases} \left[(u + \sqrt{\tau})^{\frac{1}{3}} + (u - \sqrt{\tau})^{\frac{1}{3}} \right]^2, \tau \geq 0, \\ \\ 4v \cos^2 \left[\frac{1}{3} \arccos(uv^{-\frac{3}{2}}) \right], \quad \tau < 0. \end{cases} \tag{42}$$

Then (41) has a unique solution x_-^* given by

$$x_-^* = \Pi_{B_-}(x_{\omega,\beta}^-) := \min\{\delta^2, \max\{a, \; x_{\omega,\beta}^-\}\} \quad and \quad x_-^* \geq \min\{\delta^2, \; 1, \; \gamma_{\omega,\beta}\}.$$

Proof For notational simplicity, denote $z := x_{\omega,\beta}^-$. Let us consider

$$\min \;\; q_-(x), \qquad s.t. \;\; x \geq 0. \tag{43}$$

By noticing that the second derivative $q_-''(x) = 1 + (\beta/4)x^{-2/3} > 1$ for all $x > 0$, $q_-(x)$ is strongly convex over $(0, \infty)$. It has been proved in [55, Prop. 3.1] that $z > 0$ is the optimal solution of (43). Since $q_-(x)$ is a univariate convex function, its optimal solution over B_- is the projection of z onto B_-, i.e., $x_-^* = \Pi_{B_-}(x_{\omega,\beta}^-)$.

Note that z is the optimal solution of (43) and $z > 0$. We must have $q_-'(z) = z - \omega - \beta/(2\sqrt{z}) = 0$. If $z \leq 1$ then $\sqrt{z} \geq z$, implying $\sqrt{z} - \omega - \beta/(2\sqrt{z}) \geq q_-'(z) = 0$, which is equivalent to $z \geq \gamma_{\omega,\beta} > 0$. Thus we must have $z \geq \min\{1, \gamma_{\omega,\beta}\}$ and it holds $x_-^* = \Pi_{B_-}(z) = \min\{\delta^2, \max\{a, \; z\}\} \geq \min\{\delta^2, \; 1, \; \gamma_{\omega,\beta}\}$, which is the claimed lower bound for x_-^*. □

Now we characterize the optimal solution of $q_+(x)$ over B_+.

Proposition 3 *Assume that $\beta < 4\delta^3$ and consider the optimization problem:*

$$x_+^* := \arg\min q_+(x), \qquad s.t. \;\; x \in B_+. \tag{44}$$

Define

$$x_{\omega,\beta}^+ := \begin{cases} \delta^2 & if \;\; \tau \geq 0 \\ \\ 4v^2 \cos^2 \left[\frac{1}{3} \arccos(-uv^{-3/2}) \right] & if \;\; \tau < 0, \end{cases} \tag{45}$$

Then $q_+(x)$ is strictly convex over the interval $[\delta^2, \infty)$ and

$$x_+^* = \Pi_{B_+}(x_{\omega,\beta}^+) := \max\{\delta^2, \min\{b, \; x_{\omega,\beta}^+\}\}.$$

Proof The first and the second derivatives of $q_+(x)$ are

$$q_+'(x) = x - \omega + \frac{\beta}{2\sqrt{x}}, \quad q_+''(x) = 1 - \frac{\beta}{4\sqrt{x^3}}, \quad \forall \; x > 0.$$

It is easy to verify that for $x \geq \delta^2$ and $\beta < 4\delta^3$

$$q_+''(x) \geq 1 - \frac{\beta}{4\delta^3} > 0,$$

which implies that $q(x)$ is strictly convex on $[\delta^2, \infty)$.

We consider two cases. Case 1: $\tau \geq 0$. This implies $\omega \leq 3u^{2/3}$. It follows that for $x > 0$

$$q'_+(x) = x - \omega + \frac{\beta}{4\sqrt{x}} + \frac{\beta}{4\sqrt{x}}$$

$$\geq 3\left[x\frac{\beta}{4\sqrt{x}}\frac{\beta}{4\sqrt{x}}\right]^{1/3} - \omega = 3\left[\frac{\beta^2}{4^2}\right]^{1/3} - \omega = 3u^{2/3} - \omega \geq 0.$$

This implies that $q_+(x)$ is non-decreasing and hence $x^*_+ = \delta^2$.

Case 2: $\tau < 0$, which implies $\omega > 3u^{2/3}$. Consider the problem:

$$\min \ q_+(x) \qquad \text{s.t.} \ \ x \geq 0. \tag{46}$$

We will apply Lemma 3 to the problem (46) and show that exactly one of its two positive stationary points falls within the interval $[\delta^2, \infty)$. We will further show that this stationary point is defined by (45) for the case $\tau < 0$. Since $q_+(x)$ is convex over this interval, the optimal solution of the problem (44) is just the projection of this stationary point onto the interval $B_+ = [\delta^2, b]$. This would complete the proof.

Comparing the problem (46) with the problem (34), the corresponding quantities are

$$\nu = 2\beta, \quad t = \omega, \quad \bar{x} = (\nu/8)^{2/3} = (\beta/4)^{2/3} = u^{2/3} \quad \text{and} \quad \bar{t} = 3\bar{x}.$$

It is obvious that $t = w > 3u^{2/3} = 3\bar{x}$ (the condition of Lemma 3 is satisfied). Lemma 3 implies that the problem (46) has two positive stationary points, which must satisfy the optimality condition $q'_+(\hat{x}) = 0$, leading to

$$\hat{x} - \omega + \frac{\beta}{2\sqrt{\hat{x}}} = 0.$$

Let $\hat{y} := \sqrt{\hat{x}}$, we then have

$$\hat{y}^3 - \omega\hat{y} + \frac{\beta}{2} = 0. \tag{47}$$

This is the well-known depressed cubic equation, whose solution (i.e., Cardan formula) has a long history [7, Chp. 7].

Since $\omega > 3u^{2/3}$, it follows from the Cardan formula (in terms of the trigonometric functions, see [50, Sect. 3]) that (47) has three real roots, namely

$$\hat{y}_1 := 2\sqrt{v}\cos(\theta/3), \quad \hat{y}_2 := 2\sqrt{v}\cos((4\pi + \theta)/3), \quad \hat{y}_3 := 2\sqrt{v}\cos((2\pi + \theta)/3)$$

with $\cos(\theta) = -uv^{-3/2}$. Moreover, the three roots satisfy that $\hat{y}_1 \geq \hat{y}_2 \geq \hat{y}_3$. According to Lemma 3, two of them are positive. That is, $\hat{y}_1 > 0$, $\hat{y}_2 > 0$ and

$$\hat{y}_2^2 < \bar{x} < \hat{y}_1^2.$$

Since $\beta < 4\delta^3$, we have

$$\bar{x} = u^{2/3} = (\beta/4)^{2/3} < \delta^2.$$

Therefore, $\hat{y}_1^2$ is the only point that falls within the interval $[\delta^2, \infty]$. Since $q_+(x)$ is strictly convex, the minimum of the problem (44) must be the projection of $\hat{y}_1^2$ onto the interval B_+. Hence, for the Case 2, we must have $x^*_+ = \Pi_{B_+}(\hat{y}_1^2)$. The proof is completed by noting that $\hat{y}_1^2$ is just $x^+_{\omega,\beta}$ defined in (45) for the case $\tau < 0$. $\qquad\square$

Putting together Prop. 2 and Prop. 3 gives rise to the optimal solution of (39).
The optimal solution is either x_-^* or x_+^*, whichever gives a lower functional value
of $q(x)$. This is the first result of our major theorem below. We note that both
Prop. 2 and Prop. 3 make use of the convexity of $q_-(x)$ and $q_+(x)$ on the respective
interval $[a, \delta^2]$ and $[\delta^2, b]$. In fact, we can establish a stronger result that when the
two pieces join together, the resulting function $q(x)$ is still convex on the whole
interval $[a, b]$. This result is very important to our convergence analysis in the next
section and is the second result of the theorem below. A key tool for the proof is
Lemma 1.

Theorem 1 *Let B denote the interval $[a, b]$ with $0 \leq a \leq \delta^2 \leq b$. We assume
$0 < \beta < 4\delta^3$. Then, the following hold.*

(i) The optimal solution of the problem (39) is given by

$$\mathtt{dcroot}_B[\omega, \beta, \delta] = \underset{x \in \{x_-^*,\, x_+^*\}}{\arg\min}\ q(x).$$

*(ii) The function $q(x)$ is strictly convex on $[a, b]$. Consequently, there exists $\xi \in
\partial q(\mathtt{dcroot}_B[\omega, \beta, \delta])$ such that*

$$\xi(x - \mathtt{dcroot}_B[\omega, \beta, \delta]) \geq 0 \quad \text{for any } x \in B.$$

*(iii) Let $\gamma_{\omega,\beta}$ be defined in (40), then $\mathtt{dcroot}_B[\omega, \beta, \delta] \geq \min\{\delta^2, b, 1, \gamma_{\omega,\beta}\}$. We
view $\mathtt{dcroot}_B[\omega, \beta, \delta]$ as a function of ω. Suppose $C > 0$ is an arbitrarily given
constant. Then there exists a constant $\kappa > 0$ such that*

$$\mathtt{dcroot}_B[\omega, \beta, \delta] > \kappa \quad \forall\ \omega \text{ such that } |\omega| \leq C.$$

Proof (i) is a direct consequence of Prop. 2 and Prop. 3. We now prove (ii). For
any $x, y > 0$ and any $\xi_x \in \partial q(x)$, it follows that

$$\xi_x = x - \omega + \beta\zeta \quad \text{with } \zeta \in \partial\phi_\delta(x)$$

and

$$\begin{aligned}
q(y) - q(x) &= \frac{1}{2}(y - \omega)^2 - \frac{1}{2}(x - \omega)^2 + \beta(|\sqrt{y} - \delta| - |\sqrt{x} - \delta|) \\
&= (x - \omega)(y - x) + \frac{1}{2}(x - y)^2 + \beta(|\sqrt{y} - \delta| - |\sqrt{x} - \delta|) \\
&\geq (x - \omega)(y - x) + \frac{1}{2}(x - y)^2 - \beta\zeta(x - y) - \frac{\beta(x - y)^2}{8\delta^3} \\
&= (x - \omega + \beta\zeta)(y - x) + \frac{4\delta^3 - \beta}{8\delta^3}(x - y)^2 \\
&> \xi_x(y - x),
\end{aligned}$$

where the first inequality above used Lemma 1 and the last inequality used the
fact $4\delta^3 > \beta > 0$. Swapping the role of x and y above yields

$$q(x) - q(y) > \xi_y(x - y) \quad \forall\ x, y > 0,\ \xi_y \in \partial q(y).$$

Therefore, we have

$$(\xi_x - \xi_y)(x - y) > 0 \quad \forall\ x, y > 0,\ \xi_x \in \partial q(x) \text{ and } \xi_y \in \partial q(y).$$

This together with Thm. 12.17 of [41] proves that $q(x)$ is strictly convex over $[a, b]$. The rest in (ii) is just the first order optimality condition of the convex optimization problem (39) because we just proved the convexity of $q(x)$ over $[a, b]$. Finally, we prove (iii). It follows from (40) that

$$\gamma_{\omega, \beta} = \left[\frac{\omega + \sqrt{\omega^2 + 2\beta}}{2} \right]^2 = \left[\frac{\beta}{\sqrt{\omega^2 + 2\beta} - \omega} \right]^2 \geq \left[\frac{\beta}{\sqrt{C^2 + 2\beta} + C} \right]^2 := \kappa_0$$

and from Prop. 2 and Prop. 3 that

$$x_-^* \geq \min\{\delta^2, \ 1, \ \kappa_0\} \quad \text{and} \quad x_+^* \geq \delta^2.$$

Therefore,

$$\texttt{dcroot}_B[\omega, \beta, \delta] \geq \min\{\delta^2, \ 1, \ \kappa_0\} := \kappa.$$

We finish our proof.   □

Comment: The optimal solution $\texttt{dcroot}_B[\omega, \beta, \delta]$ is unique, since $q(x)$ is strictly convex over $[a, b]$. However, its location could be within the interval $[a, \sigma^2]$ or $[\sigma^2, b]$, depending on the magnitudes of the parameters (ω, β and δ) involved. The dependence is illustrated in Fig. 1. We also note that the function $q(x)$ may not be convex if the condition $\beta < 4\delta^3$ is violated.   □
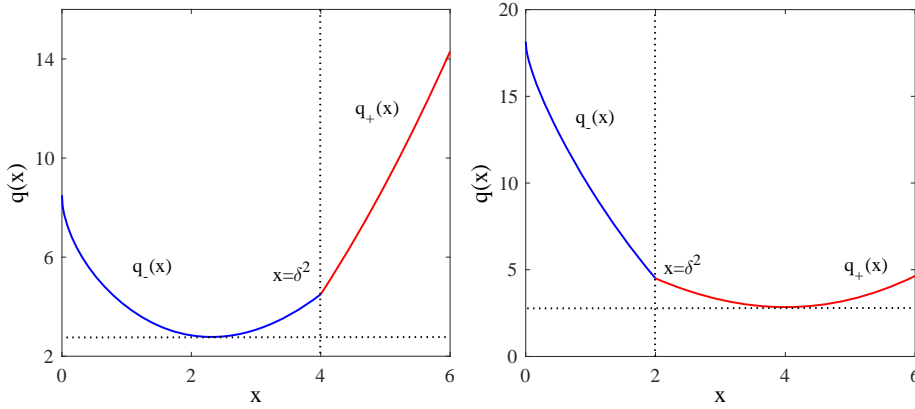
Fig. 1: Illustration of the convexity of $q(x) = 0.5(x - \omega)^2 + \beta|\sqrt{x} - \delta|$ over the interval $[0, 6]$ and $\beta = 4$: Global minimum happens on $q_-(x)$ (left) with $\omega = 1$, $\delta = 2$ and global minimum happens on $q_+(x)$ (right) with $\omega = 5$, $\delta = \sqrt{2}$.

It now follows from Thm. 1 that the optimal solution Z_{ij}^+ in (37) can be computed by:

$$Z_{ij}^+ = \begin{cases} \texttt{dcroot}_{[L_{ij}, U_{ij}]}[(Z_K)_{ij}, \ W_{ij}/\rho, \ \delta_{ij}], & W_{ij} > 0 \\ \Pi_{[L_{ij}, U_{ij}]}((Z_K)_{ij}), & W_{ij} = 0 \end{cases} \tag{48}$$

Consequently, $Z^+ = \texttt{PREEEDM}_\mathcal{B}(Z_K, W/\rho, \Delta)$ in (38) is well defined and its elements can be computed by (48).

5 Algorithm `PREEEDM` and Its Convergence

With the preparations above, we are ready to state our algorithm. Let $D^k \in \mathcal{B}$ be the current iterate. We update it by solving the majorization subproblem of the type (36) with Z replaced by D^k:

$$D^{k+1} = \arg\min \left\{ f_\rho^k(D) := f(D) + \rho g_m(D, D^k) \right\}, \text{ s.t. } D \in \mathcal{B}, \qquad (49)$$

which can be computed by

$$D^{k+1} = \texttt{REEEDM}_\mathcal{B}(-\Pi_{\mathcal{K}_+^n(r)}(-D^k), \ W/\rho, \ \Delta). \qquad (50)$$

In more detail, we have

$$f_\rho^k(D) = \|W \circ (\sqrt{D} - \Delta)\|_1 + \frac{\rho}{2}\|D + \Pi_{\mathcal{K}_+^n(r)}(-D^k)\|^2$$

$$= \sum_{i,j} \underbrace{\left[\frac{\rho}{2}\Big(D_{ij} - (Z_K^k)_{ij} \Big)^2 + W_{ij}|\sqrt{D_{ij}} - \delta_{ij}| \right]}_{=:f_{ij}^k(D_{ij})}$$

where $Z_K^k := -\Pi_{\mathcal{K}_+^n(r)}(-D^k)$, and the elements of D^{k+1} are computed as follows:

$$D_{ij}^{k+1} = \underset{L_{ij} \leq D_{ij} \leq U_{ij}}{\operatorname{argmin}} \left\{ \frac{1}{2}\Big[D_{ij} - (Z_K^k)_{ij} \Big]^2 + \frac{W_{ij}}{\rho}\Big| \sqrt{D_{ij}} - \delta_{ij} \Big| \right\}$$

$$= \begin{cases} \texttt{dcroot}_{[L_{ij}, U_{ij}]}\Big[(Z_K^k)_{ij}, \ W_{ij}/\rho, \ \delta_{ij} \Big], & \text{if } W_{ij} > 0 \\[2mm] \Pi_{[L_{ij}, U_{ij}]}\Big[(Z_K^k)_{ij} \Big], & \text{if } W_{ij} = 0. \end{cases} \qquad (51)$$

Our algorithm `PREEEDM` is formally stated as follows.

Algorithm 1 `PREEEDM` Method

1: **Input data:** Dissimilarity matrix Δ, weight matrix W, penalty parameter $\rho > 0$, lower-bound matrix L, upper-bound matrix U and the initial D^0. Set $k := 0$.
2: **Update:** $D^{k+1} = \texttt{PREEEDM}_\mathcal{B}(-\Pi_{\mathcal{K}_+^n(r)}(-D^k), \ W/\rho, \ \Delta)$ by (51).
3: **Convergence check:** Set $k := k + 1$ and go to Step 2 until convergence.

A major obstacle in analysing the convergence for the penalized EDM model (16) is the non-differentiability of the objective function. We need the following two reasonable assumptions:

Assumption 1: The constrained box $\mathcal{B}$ is bounded.

Assumption 2: For Δ and U, we require $W_{ij} = 0$ if $\delta_{ij} = 0$ and $U_{ij} \geq \delta_{ij}^2 \geq L_{ij}$ if $\delta_{ij} > 0$

Assumption 1 can be easily satisfied (e.g., setting the upper bound to be $n^2 \max\{\delta_{ij}^2\}$). Assumption 2 means that if $\delta_{ij} = 0$ (e.g., value missing), the corresponding weight W_{ij} should be 0. This is a common practice in applications.

If $\delta_{ij} > 0$, then we require δ_{ij}^2 to be between L_{ij} and U_{ij}. We further define a quantity that bounds our penalty parameter ρ from below:

$$\rho_o := \rho_o(W, \Delta) := \max_{(i,j):W_{ij}>0} \frac{W_{ij}}{4\delta_{ij}^3} \qquad (52)$$

Our first result in this section is about the boundedness of the subdifferential of $f(\cdot)$ along the generated sequence $\{D^k\}$.

Proposition 4 *Suppose Assumptions 1 and 2 hold. Let $\rho > \rho_o$ and $\{D^k\}$ be the sequence generated by Alg. 1. Then the following hold.*

(i) There exists a constant $c_1 > 0$ such that

$$D_{ij}^k \geq c_1 \qquad \text{for all } (i,j) \text{ such that } W_{ij} > 0 \text{ and } k = 1, 2, \ldots.$$

(ii) Let $\partial f(D)$ denote the subdifferential of $f(D) = \|W \circ (\sqrt{D} - \Delta)\|_1$. Then there exists a constant $c_2 > 0$ such that

$$\|\Gamma\| \leq c_2 \qquad \forall \ \Gamma \in \partial f(D^k), \quad k = 1, 2, \ldots.$$

(iii) The function $f_\rho^k(D)$ is convex for all $k = 1, 2, \ldots$. Moreover, there exists $\Gamma^{k+1} \in \partial f(D^{k+1})$ such that the first-order optimality condition for (50) is

$$\left\langle \Gamma^{k+1} + \rho D^{k+1} + \rho \Pi_{\mathcal{K}_+^n(r)}(-D^k), \ D - D^{k+1} \right\rangle \geq 0, \qquad \forall \ D \in \mathcal{B}. \quad (53)$$

Proof (i) Let us pick a pair (i,j) such that $W_{ij} > 0$, which implies $\delta_{ij} > 0$ (Assumption 2). It follows from (51) that

$$D_{ij}^k = \texttt{dcroot}_{[L_{ij}, U_{ij}]}\left[(Z_K^{k-1})_{ij}, \ W_{ij}/\rho, \ \delta_{ij}\right],$$

where $Z_K^{k-1} := -\Pi_{\mathcal{K}_+^n(r)}(-D^{k-1})$. Since $\mathcal{B}$ is bounded (Assumption 1) and $D^k \in \mathcal{B}$, the sequence $\{D^k\}$ is bounded. Lemma 2 implies

$$\| - \Pi_{\mathcal{K}_+^n(r)}(-D^{k-1})\| \leq 2\|D^{k-1}\| \leq 2\|U\|,$$

which further implies $|(Z_K^{k-1})_{ij}| \leq 2\|U\|$ for all $k = 1, \ldots$. Let $\beta_{ij} := W_{ij}/\rho$. Then

$$0 < \beta_{ij} < 4\delta_{ij}^3$$

owing to $\rho > \rho_o(W, \Delta)$. It follows from Thm. 1(iii) that there exists $\kappa_{ij} > 0$ such that $D_{ij}^k \geq \kappa_{ij}$ for all $k = 1, 2, \ldots,$. The choice of c_1 by

$$c_1 := \min\{\kappa_{ij} : \ (i,j) \text{ such that } W_{ij} > 0\} > 0.$$

satisfies the bound in (i).

(ii) We write $f(D)$ in terms of D_{ij}:

$$f(D) = \sum_{i,j} W_{ij}|\sqrt{D_{ij}} - \delta_{ij}| = \sum_{i,j} W_{ij}\phi_{\delta_{ij}}(D_{ij}). \qquad (54)$$

We let $\partial_{ij}f(D)$ denote the subdifferential of f with respect to its $(i,j)th$ element D_{ij}. We consider two cases. **Case 1**: $W_{ij} = 0$. This implies that $f(D)$ is a constant

function ($\equiv 0$) of D_{ij} and hence $f(D)$ is continuously differentiable with respect to D_{ij}. Consequently, $\partial_{ij} f(D^k) = \{0\}$.

Case 2: $W_{ij} > 0$, which implies $\delta_{ij} > 0$ (Assumption 2). It follows from (i) that there exists $c_1 > 0$ such that $D_{ij}^k \geq c_1$ for all $k = 1, 2, \ldots,$. The equations (54) and (25) yield

$$\partial_{ij} f(D^k) = W_{ij} \text{sign}\left[\sqrt{D_{ij}^k} - \delta_{ij}\right] \Big/ \left[2\sqrt{D_{ij}^k}\right],$$

which implies that for any $\xi_{ij}^k \in \partial_{ij} f(D^k)$ there exists $\zeta_{ij}^k \in \text{sign}((D_{ij}^k)^{1/2} - \delta_{ij})$ such that

$$|\xi_{ij}^k| = W_{ij} |\zeta_{ij}^k| \Big/ \left[2\sqrt{D_{ij}^k}\right] \leq W_{ij}/\sqrt{4c_1}.$$

In other words, $\partial_{ij} f(D^k)$ is bounded by $W_{ij}/\sqrt{c_1}$, which is independent of the index k. It follows directly from the definition of subdifferential [41, Chp. 8.3] that

$$\partial f(D^k) \subseteq \bigotimes \partial_{ij} f(D^k)$$

in the sense that for any $\Gamma^k \in \partial f(D^k)$, there exist $\xi_{ij}^k \in \partial_{ij} f(D^k)$ such that

$$\Gamma_{ij}^k = \xi_{ij}^k, \qquad i, j = 1, \ldots, n.$$

Consequently, we have for all $k = 1, 2, \ldots,$

$$\|\Gamma^k\| \leq n \max_{i,j} |\xi_{ij}^k| \leq n W_{ij}/(2\sqrt{c_1}) \leq n \max_{i,j} W_{ij}/(2\sqrt{c_1}) =: c_2 > 0.$$

This completes the proof for (ii).

(iii) Since $\rho > \rho_o$, for each pair (i,j) we have $\beta_{ij} := W_{ij}/\rho < 4\delta_{ij}^3$. It then follows from Thm. 1(ii) that each separable function $f_{ij}^k(D_{ij})$ is convex and hence the function $f_\rho^k(D)$ is convex over $D \in \mathcal{B}$. Consequently, subproblem (49) is convex. The first-order necessary and sufficient optimality condition is just (53). $\square$

Thm. 1(i) ensures that $D_{ij}^k > 0$ for all $k = 1, \ldots,$. Hence, we can apply Lem. 1 to each function $\phi_{\delta_{ij}}(\cdot)$ with $x = D_{ij}^{k+1}$ and $y = D_{ij}^k$. This yields for any $\zeta_{ij}^{k+1} \in \partial \phi_{\delta_{ij}}(D_{ij}^{k+1})$

$$\phi_{\delta_{ij}}(D_{ij}^{k+1}) - \phi_{\delta_{ij}}(D_{ij}^k) \leq \zeta_{ij}^{k+1}(D_{ij}^{k+1} - D_{ij}^k) + \frac{1}{2} \frac{(D_{ij}^{k+1} - D_{ij}^k)^2}{4\delta_{ij}^3},$$

Multiplying W_{ij} on both sides and adding those inequalities over (i,j), we get

$$f(D^{k+1}) - f(D^k) \leq \langle \Gamma^{k+1}, D^{k+1} - D^k \rangle + \frac{\rho_o}{2} \|D^{k+1} - D^k\|^2, \qquad (55)$$

where $\Gamma_{ij}^{k+1} := W_{ij} \zeta_{ij}^{k+1}$. We note that the inequality (55) holds for any $\Gamma^{k+1} \in \partial f(D^{k+1})$.

Theorem 2 *Let $\rho > \rho_o$ and $\{D^k\}$ be the sequence generated by Alg. 1. Suppose Assumptions 1 and 2 hold.*

(i) We have

$$f_\rho(D^{k+1}) - f_\rho(D^k) \leq -\frac{\rho - \rho_o}{2}\|D^{k+1} - D^k\|^2 \quad for \ any \ \ k = 0, 1, \ldots, .$$

Consequently, $\|D^{k+1} - D^k\| \to 0$.

(ii) Let $\widehat{D}$ be an accumulation point of $\{D^k\}$. Then there exists $\widehat{\Gamma} \in \partial f(\widehat{D})$ such that

$$\langle \widehat{\Gamma} + \rho\widehat{D} + \rho\Pi_{\mathcal{K}_+^n(r)}(-\widehat{D}), \ D - \widehat{D} \rangle \geq 0 \quad for \ any \ D \in \mathcal{B}. \qquad (56)$$

That is, $\widehat{D}$ is a stationary point of the problem (16).

(iii) If $\widehat{D}$ is an isolated accumulation point of the sequence $\{D^k\}$, then the whole sequence $\{D^k\}$ converges to $\widehat{D}$.

Proof (i) We are going to use the following facts that are stated on D^{k+1} and D^k. The first fact is the identity:

$$\|D^{k+1}\|^2 - \|D^k\|^2 = 2\langle D^{k+1} - D^k, \ D^{k+1} \rangle - \|D^{k+1} - D^k\|^2. \qquad (57)$$

The second fact is due to the convexity of $h(D)$ (see Lemma 2(ii)):

$$h(-D^{k+1}) - h(-D^k) \geq \langle \Pi_{\mathcal{K}_+^n(r)}(-D^k), \ -D^{k+1} + D^k \rangle. \qquad (58)$$

The last fact is that there exists $\Gamma^{k+1} \in \partial f(D^{k+1})$ such that (53). Those facts yield the following chain of inequalities:

$$
\begin{aligned}
&f_\rho(D^{k+1}) - f_\rho(D^k) \\
=\ & f(D^{k+1}) - f(D^k) + \rho g(D^{k+1}) - \rho g(D^k) \\
\overset{(55)}{\leq}\ & \langle \Gamma^{k+1}, \ D^{k+1} - D^k \rangle + \frac{\rho_o}{2}\|D^{k+1} - D^k\|^2 + \rho g(D^{k+1}) - \rho g(D^k) \\
\overset{(32)}{=}\ & \langle \Gamma^{k+1}, \ D^{k+1} - D^k \rangle + \frac{\rho_o}{2}\|D^{k+1} - D^k\|^2 \\
&+\ (\rho/2)(\|D^{k+1}\|^2 - \|D^k\|^2) - \rho[h(-D^{k+1}) - h(-D^k)] \\
\overset{(57)}{=}\ & \langle \Gamma^{k+1} + \rho D^{k+1}, \ D^{k+1} - D^k \rangle \\
&-\ \frac{\rho - \rho_o}{2}\|D^{k+1} - D^k\|^2 - \rho[h(-D^{k+1}) - h(-D^k)] \\
\overset{(58)}{\leq}\ & \langle \Gamma^{k+1} + \rho D^{k+1} + \rho\Pi_{\mathcal{K}_+^n(r)}(-D^k), \ D^{k+1} - D^k \rangle - \frac{\rho - \rho_o}{2}\|D^{k+1} - D^k\|^2 \\
\overset{(53)}{\leq}\ & -\frac{\rho - \rho_o}{2}\|D^{k+1} - D^k\|^2.
\end{aligned}
$$

This proves that the sequence $\{F_\rho(D^k)\}$ is non-increasing and it is also bounded below by 0. Taking the limits on both sides yields $\|D^{k+1} - D^k\| \to 0$.

(ii) Suppose $\widehat{D}$ is the limit of a subsequence $\{D^{k_\ell}\}$, $\ell = 1, \ldots, .$ Since we have established in (i) that $(D^{k_\ell+1} - D^{k_\ell}) \to 0$, the sequence $\{D^{k_\ell+1}\}$ also converges to $\widehat{D}$. Furthermore, there exist a sequence of $\Gamma^{k_\ell+1} \in \partial f(D^{k_\ell+1})$ such that (53) holds. Prop. 4(ii) ensures that there exists a constant $c_2 > 0$ such that $\|\Gamma^{k_\ell+1}\| \leq c_2$ for all k_ℓ. Hence, there exists a subsequence of $\{k_\ell\}$ (we still denote the subsequence by $\{k_\ell\}$ for simplicity) such that $\Gamma^{k_\ell+1}$ converges to some $\widehat{\Gamma} \in \partial f(\widehat{D})$. Now taking the limits on both sides of (53) on $\{k_\ell\}$, we reach the desired inequality (56).

(iii) We note that we have proved in (i) that $(D^{k+1} - D^k) \to 0$. The convergence of the whole sequence to $\widehat{D}$ follows from [26, Prop. 7]. $\qquad\square$

6 Numerical Experiments

In this part, we will conduct extensive numerical experiments of our algorithm
PREEEDM by using MATLAB (R2014a) on a desktop of 8GB memory and Inter(R)
Core(TM) i5-4570 3.2Ghz CPU, against 6 leading solvers on the problems of sensor
network localizations (SNL) in $\Re^2$ ($r = 2$) and Molecular Conformation (MC) in
$\Re^3$ ($r = 3$). This section is split into the following parts. Our implementation
of PREEEDM was described in Subsect. 6.1. In Subsect. 6.2, we describe how the
test data of SNL and MC were collected and generated. We will give a brief
explanation how the six benchmark methods were selected in Subsect. 6.3. Our
extensive numerical comparisons are reported in Subsect. 6.4.

6.1 Implementation

The PREEEDM Alg. 1 is easy to implement. We first address the issue of its stopping
criterion that is to be used in Step 3 of Alg. 1. We monitor two quantities. One
is on how close of the current iterate D^k is to be Euclidean (belonging to $\mathcal{K}_+^n(r)$).
This can be computed by using (30) as follows.

$$
\begin{aligned}
\mathtt{Kprog}_k := \frac{2g(D^k)}{\|JD^kJ\|^2} &= \frac{\|\mathrm{PCA}_r^+(-JD^kJ) + (JD^kJ)\|^2}{\|JD^kJ\|^2} \\
&= 1 - \frac{\sum_{i=1}^r \left[\lambda_i^2 - (\lambda_i - \max\{\lambda_i, 0\})^2\right]}{\lambda_1^2 + \ldots + \lambda_n^2} \\
&\leq 1,
\end{aligned}
$$

where $\lambda_1 \geq \lambda_2 \geq \ldots \geq \lambda_n$ are the eigenvalues of $(-JD^kJ)$. The smaller $\mathtt{Kprog}_k$ is,
the closer D^k is to $\mathcal{K}_+^n(r)$. The benefit of using $\mathtt{Kprog}$ over $g(D)$ is that the former
is independent of any scaling of D.

   The other quantity is to measure the progress in the functional values $f_\rho(\cdot)$
by the current iterate D^k. In theory (see Thm. 2), we should require $\rho > \rho_o$,
which is defined as (52) and is potentially large. As with the most penalty meth-
ods [33, Chp. 17], starting with a very large penalty parameter may degrade the
performance of the method (e.g., causing air-conditionness). We adopt a dynamic
updating rule for ρ. In particular, we choose $\rho_0 = \frac{\kappa \max \delta_{ij}}{n^{3/2}}$ and update it as

$$
\rho_{k+1} = \begin{cases}
1.25\rho_k, & \text{if } \mathtt{Kprog}_k > \mathtt{Ktol}, \mathtt{Fprog}_k \leq 0.2\mathtt{Ftol}, \\
0.75\rho_k, & \text{if } \mathtt{Fprog}_k > \mathtt{Ftol}, \mathtt{Kprog}_k \leq 0.2\mathtt{Ktol}, \\
\rho_k, & \text{otherwise,}
\end{cases}
$$

where

$$
\mathtt{Fprog}_k := \frac{f_{\rho_{k-1}}(D^{k-1}) - f_{\rho_{k-1}}(D^k)}{1 + \rho_{k-1} + f_{\rho_{k-1}}(D^{k-1})}, \tag{59}
$$

and $\mathtt{Ftol} = \ln(\kappa) \times 10^{-4}$ and $\mathtt{Ktol} = 10^{-2}$ with κ being the number of non-zero
elements of Δ. We terminate PREEEDM when

$$
\mathtt{Fprog}_k \leq \mathtt{Ftol} \quad \text{and} \quad \mathtt{Kprog}_k \leq \mathtt{Ktol},
$$

Since our computation of each iteration is dominated by $\Pi_{\mathcal{K}^n_+(r)}(-D)$ in the construction of the majorization function $g_m(\cdot,\cdot)$ in (33), the computational complexity is about $O(rn^2)$ (we used MATLAB's built-in function `eigs.m` to compute $\text{PCA}^+_r(A)$ in (29)). For the problem data input, Δ, L and U will be described in Subsect. 6.2. For the initial point, we follow the popular choice used in [43, 46] $\sqrt{D^0} := \widehat{\Delta}$, where $\widehat{\Delta}$ is the matrix obtained by the shortest path distances among Δ. If Δ has no missing values, then $\widehat{\Delta} = \Delta$.

6.2 Test examples

Our test data comes from the problem of sensor network localization (SNL) and the molecular conformation (MC). SNL has been widely used to test the viability of many existing methods for the stress minimization. In such a problem, we typically have m anchors (e.g., sensors with known locations) and the rest sensors need to be located. We will test two types of SNL problems. One has a regular topological layout (Examples 1 and 2 below). The other has an irregular layout (Example 3).

Example 1 (Square Network with 4 fixed anchors) This example is widely tested since its detailed study in [5]. In the square region $[-0.5, 0.5]^2$, 4 anchors $\mathbf{x}_1 = \mathbf{a}_1, \cdots, \mathbf{x}_4 = \mathbf{a}_4$ ($m = 4$) are placed at $(\pm 0.2, \pm 0.2)$. The generation of the rest $(n - m)$ sensors $(\mathbf{x}_{m+1}, \cdots, \mathbf{x}_n)$ follows the uniform distribution over the square region. The noisy Δ is usually generated as follows.

$$\delta_{ij} := \|\mathbf{x}_i - \mathbf{x}_j\| \times |1 + \epsilon_{ij} \times \mathtt{nf}|, \ \forall \ (i,j) \in \mathcal{N} := \mathcal{N}_x \cup \mathcal{N}_a$$
$$\mathcal{N}_x := \{(i,j) \mid \|\mathbf{x}_i - \mathbf{x}_j\| \le R, \ i > j > m\}$$
$$\mathcal{N}_a := \{(i,j) \mid \|\mathbf{x}_i - \mathbf{a}_j\| \le R, \ i > m, \ 1 \le j \le m\},$$

where R is known as the radio range, ϵ_{ij}'s are independent standard normal random variables, and $\mathtt{nf}$ is the noise factor (e.g., $\mathtt{nf} = 0.1$ was used and it corresponds to 10% noise level). In literature (e.g., [5]), this type of perturbation in δ_{ij} is known to be multiplicative and follows the unit-ball rule in defining $\mathcal{N}_x$ and $\mathcal{N}_a$ (see [3, Sect. 3.1] for more detail). The corresponding weight matrix W and the lower and upper bound matrices L and U are given as in the table below. Here, M is a large positive quantity. For example, $M := n \max_{ij} \Delta_{ij}$ is the upper bound of the longest shortest path if the network is viewed as a graph.

(i,j)	W_{ij}	Δ_{ij}	L_{ij}	U_{ij}
$i = j$	0	0	0	0
$i, j \le m$	0	0	$\|\mathbf{a}_i - \mathbf{a}_j\|^2$	$\|\mathbf{a}_i - \mathbf{a}_j\|^2$
$(i,j) \in \mathcal{N}$	1	δ_{ij}	0	R^2
otherwise	0	0	R^2	M^2

Example 2 (Square Network with m random anchors) This example also tested in [5] is similar to Example 1 but with randomly generated anchors. The generation of n points follows the uniform distribution over the square region $[-0.5, 0.5]^2$. Then the first m points are chosen to be anchors and the last $(n - m)$ points to be sensors. The rest of the data generation is same as in Example 1.

Example 3 (EDM word network) This problem has a non-regular topology and was first used in [3] to challenge existing methods. In this example, n points are randomly generated in a region whose shape is similar to the letters "E", "D" and "M". The ground truth network is depicted in Fig. 2. We choose the first m points to be the anchors. The rest of the data generation is same as in Example 1.
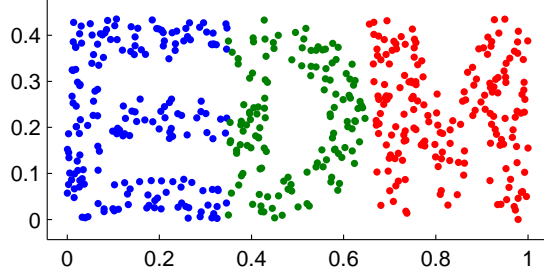
Fig. 2: Ground truth EDM network with $n = 500$ nodes.

MC has long been an important application of EDM optimization [2,21,32]. We will test two types of MCs respectively from an artificial data set and a real data set in Protein Data Bank (PDB) [4]. For the former, we adopt the rule of generating data from [2,32]. For the latter, we used the real data of 12 molecules derived from 12 structures of proteins from PDB. They are `1GM2`, `304D`, `1PBM`, `2MSJ`, `1AU6`, `1LFB`, `104D`, `1PHT`, `1POA`, `1AX8`, `1RGS`, `2CLJ`. They provide a good set of test problems in terms of the size n, which ranges from a few hundreds to a few thousands (the smallest $n = 166$ for `1GM` and the largest $n = 4189$ for `2CLJ`). The distance information was obtained in a realistic way as done in [24].

Example 4 (Artificial data) As described in [2,32], the artificial molecule has $n = s^3$ atoms $(\mathbf{x}_1, \cdots, \mathbf{x}_n)$ located in the three-dimensional lattice

$$\{(i_1, i_2, i_3) : i_1, i_2, i_3 = 0, 1, \ldots, s-1\}$$

for some integer $s \geq 1$, i.e., $\mathbf{x}_i = (i_1, i_2, i_3)^T$. We define $\mathcal{N}_x$ for the index set on which δ_{ij} are available as:

$$\mathcal{N}_x := \{(i,j) : |p(\mathbf{x}_i) - p(\mathbf{x}_j)| \leq R\} \tag{60}$$

where $p(\mathbf{x}_i) := 1 + (1, s, s^2)^T \mathbf{x}_i = 1 + i_1 + s i_2 + s^2 i_3$ and R is a given constant (e.g., $R = s^2$). The corresponding dissimilarity matrix Δ, weight matrix W and the lower and upper bound matrices L and U are given as in the table below. Here the generation of δ_{ij} is the same as Example 1.

(i,j)	W_{ij}	Δ_{ij}	L_{ij}	U_{ij}
$i = j$	0	0	0	0
$(i,j) \in \mathcal{N}_x$	1	δ_{ij}	1	$\max_{(i,j)\in\mathcal{N}_x} \|\mathbf{x}_i - \mathbf{x}_j\|^2$
otherwise	0	0	1	$3(s-1)^2$

Example 5 (Real PDB data) Each molecule comprises n atoms $\{\mathbf{x}_1, \ldots \mathbf{x}_n\}$ in $\Re^3$ and its distance information is collected as follows. If the Euclidean distance between two of the atoms is less than R, the distance is chosen; otherwise no distance information about this pair is known. For example, $R = 6\mathring{A}$ $(1\mathring{A} = 10^{-8}\text{cm})$ is nearly the maximal distance that the nuclear magnetic resonance (NMR) experiment can measure between two atoms. For realistic molecular conformation problems, not all the distances below R are known from NMR experiments, so one may obtain $c\%$ (e.g., $c = 50\%$) of all the distances below R. Denote $\mathcal{N}_x$ the set formed by indices of those measured distances. Moreover, the distances in $\mathcal{N}_x$ can not be exactly measured. Instead, only lower bounds ℓ_{ij} and upper bounds u_{ij} are provided, that is for $(i, j) \in \mathcal{N}_x$,

$$\ell_{ij} = \max\left\{1, (1 - |\epsilon_{ij}|)\|\mathbf{x}_i - \mathbf{x}_j\|\right\}, \quad u_{ij} = (1 + |\varepsilon_{ij}|)\|\mathbf{x}_i - \mathbf{x}_j\|.$$

where $\epsilon_{ij}, \varepsilon_{ij} \sim N(0, \mathtt{nf}^2 \times \pi/2)$ are independent normal random variables. In our test, we set the noise factor $\mathtt{nf} = 0.1$ and the parameters $W, \Delta, L, U \in \mathcal{S}^n$ are given as in the table below, where $M > 0$ is the upper bound (e.g., $M := n \max_{ij} \Delta_{ij}$).

(i, j)	W_{ij}	Δ_{ij}	L_{ij}	U_{ij}
$i = j$	0	0	0	0
$(i, j) \in \mathcal{N}_x$	1	$(\ell_{ij} + u_{ij})/2$	ℓ_{ij}^2	u_{ij}^2
otherwise	0	0	0	M^2

To assess the embedding quality, we adopt a widely used measure $\mathtt{RMSD}$ (Root of the Mean Squared Deviation) defined by

$$\mathtt{RMSD} := \left[\frac{1}{n - m} \sum_{i=m+1}^{n} \|\widehat{\mathbf{x}}_i - \mathbf{x}_i\|^2\right]^{1/2},$$

where $\mathbf{x}_i$'s are the true positions of the sensors or atoms in our test problems and $\widehat{\mathbf{x}}_i$'s are their corresponding estimates. The $\widehat{\mathbf{x}}_i$'s were obtained by applying the classical MDS ($\mathtt{cMDS}$) method to the final output of the distance matrix, followed by aligning them to the existing anchors through the well-known Procrustes procedure (see [53], [6, Chp. 20] or [40, Prop. 4.1] for more details). Furthermore, upon obtaining $\widehat{\mathbf{x}}_i$'s, a heuristic gradient method can be applied to improve their accuracy and it is called the refinement step in [5]. We report $\mathtt{rRMSD}$ to highlight its contribution. As we will see, all tested methods benefit from this step, but with varying degrees.

6.3 Benchmark methods

We select six representative state-of-the-art methods for comparison. They are $\mathtt{ADMMSNL}$ [36], $\mathtt{ARAP}$ [53], $\mathtt{EVEDM}$ (short for $\mathtt{EepVecEDM}$) [12], $\mathtt{PC}$ [1], $\mathtt{PPAS}$ (short for $\mathtt{PPA}$ $\mathtt{Semismooth}$) [24] and $\mathtt{SFSDP}$ [27]. Those methods have been shown to be capable of returning satisfactory localization/embedding in many applications. We will compare our method $\mathtt{PREEEDM}$ with $\mathtt{ADMMSNL}$, $\mathtt{ARAP}$, $\mathtt{EVEDM}$, $\mathtt{PC}$ and $\mathtt{SFSDP}$ for SNL

problems and with `EVEDM`, `PC`, `PPAS` and `SFSDP` for MC problems since the current implementations of `ADMMSNL`, `ARAP` do not support the embedding for $r \geq 3$.

We note that `ADMMSNL` is motivated by [44] and aims to enhance the package `diskRelax` of [44] for the SNL problems ($r = 2$). Both methods are based on the stress minimization (5). As we mentioned before, `SMACOF` [13,14] has been a very popular method for (5). However, we are not to compare it with other methods here since its performance demonstrated in [53,55] was not very satisfactory (e.g., when comparing with `ARAP`) for either SNL or MC problems. To our best knowledge, `PC` is the only viable method, whose code is also publicly available for the model (3). We select `SFSDP` and `PPAS` because of their high reputation in the field of SDP and quadratic SDP in returning quality localizations and conformations. We note that `SFSDP` is for the model (5) and `PPAS` is for the model (6). Finally, the method `EVEDM` is a latest method for the model (6).

In our tests, we used all of their default parameters except one or two in order to achieve the best results. In particular, for `PC`, we terminate it when $|f(D^{k-1}) - f(D^k)| < 10^{-4} \times f(D^k)$ and set its initial point to be the embedding by `cMDS` on Δ. For `SFSDP` which is a high-level MATLAB implementation of the SDP approach initiated in [49], we set `pars.SDPsolver = "sedumi"` because it returns the best overall performance. In addition, we set `pars.objSW = 1` when $m > r + 1$ and $= 3$ when $m = 0$. For `ARAP`, in order to speed up the termination, we let `tol = 0.05` and `IterNum = 20` to compute its local neighbour patches. Numerical performance demonstrated that `ARAP` could yield satisfactory embedding, but would take very long time for some examples with large n.

6.4 Numerical Comparison

In this section, we report our extensive numerical experiments and comparison on the test data described in Subsect. 6.2. The quality of the general performance of each method can be better appreciated through visualizing their key indicators: RMSD, `rRMSD`, `rTime` (time for the refinement step) and the CPU `Time` (in seconds) which is the total time including `rTime`. Hereafter, for all examples, we test 20 randomly generated instances for each case $(n, m, R, \texttt{nf})$ in SNL or each case $(n, R, \texttt{nf})$ in MC, and record the average results.

6.4.1 Comparison on SNL

a) Effect of the radio range R. It is easy to see that the radio range R decides the amount of missing dissimilarities among all elements of Δ. The smaller R is, the more numbers of δ_{ij} are unavailable, leading to more challenging problems. Therefore, we first demonstrate the performance of each method to the radio range R. For Example 1, we fix $n = 200, m = 4, \texttt{nf} = 0.1$, and alter the radio range R among $\{0.2, 0.4, \cdots, 1.4\}$. The average results were demonstrated in Figure 3. It can be seen that `ARAP` and `PREEEDM` were joint winners in terms of both RMSD and `rRMSD`. However, the time used by `ARAP` was the longest. When R became bigger than 0.6, `ADMMSNL`, `SFSDP` and `EVEDM` produced similar `rRMSD` as `ARAP` and `PREEEDM`, while the time consumed by `ADMMSNL` was significantly larger than that by `SFSDP`, `EVEDM` and `PREEEDM`. By contrast, `PC` only worked well when $R \geq 1$.
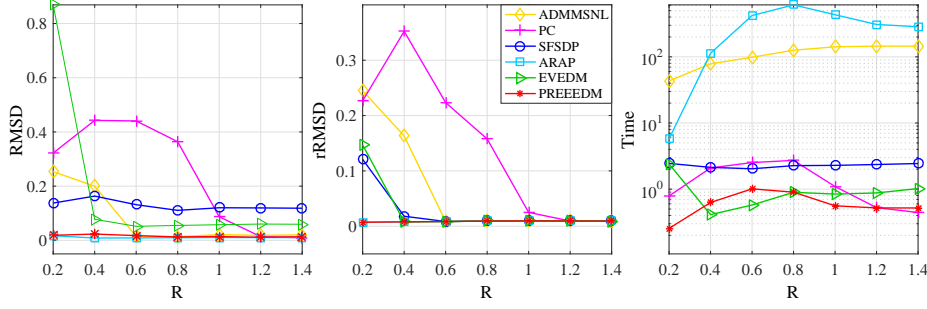
Fig. 3: Average results for Example 1 with $n = 200, m = 4$, nf $= 0.1$.

Table 1: Comparison of six methods for Example 1 with $m = 4$, nf $= 0.1$. Results of ADMMSNL when $R = \sqrt{2}$ were omitted sine it made our desktop ran out of memory. We omitted some results of ARAP because it consumed too much time.

	n		ADMMSNL	PC	SFSDP	ARAP	EVEDM	PREEEDM
		RMSD	2.07e-2	8.31e-3	1.21e-1	1.01e-2	5.95e-2	1.11e-2
	300	rRMSD	7.82e-3	7.86e-3	7.89e-3	7.96e-3	7.93e-3	7.80e-3
		rTime	3.63	0.66	3.87	0.94	3.35	1.06
		Time	348.13	1.36	6.79	503.86	3.84	1.36
		RMSD	——	6.11e-3	1.19e-1	7.51e-3	5.87e-2	8.46e-3
	500	rRMSD	——	5.94e-3	5.96e-3	6.04e-3	6.70e-3	6.11e-3
		rTime	——	1.37	14.79	3.26	13.35	3.92
$R=\sqrt{2}$		Time	——	3.83	20.22	2479.8	14.44	4.41
		RMSD	——	4.46e-3	1.25e-1	——	5.81e-2	6.59e-3
	1000	rRMSD	——	4.15e-3	7.34e-3	——	6.53e-3	4.59e-3
		rTime	——	3.51	83.96	——	68.06	9.75
		Time	——	23.05	103.29	——	71.52	10.85
		RMSD	——	3.30e-3	1.20e-1	——	5.92e-2	4.57e-3
	2000	rRMSD	——	3.10e-3	7.82e-3	——	1.24e-2	3.37e-3
		rTime	——	12.74	282.88	——	258.97	13.04
		Time	——	143.41	398.87	——	271.91	18.49
		RMSD	3.48e-1	4.42e-1	1.93e-1	4.02e-2	6.81e+1	1.88e-2
	300	rRMSD	3.33e-1	3.12e-1	1.73e-1	6.83e-3	1.72e-1	6.84e-3
		rTime	0.50	0.44	0.41	0.36	0.48	0.36
		Time	84.19	2.37	3.45	24.11	0.56	0.47
		RMSD	3.53e-1	4.30e-1	2.02e-1	1.95e-2	1.52e-1	1.77e-2
	500	rRMSD	3.35e-1	3.11e-1	1.80e-1	5.57e-3	5.59e-2	5.51e-3
		rTime	1.11	1.15	1.06	0.80	1.11	0.92
$R=0.2$		Time	156.76	5.50	6.90	161.04	1.30	1.23
		RMSD	3.62e-1	4.54e-1	1.79e-1	9.96e-3	7.21e-2	1.46e-2
	1000	rRMSD	3.44e-1	3.16e-1	1.28e-1	3.57e-3	4.06e-3	3.83e-3
		rTime	5.58	5.58	5.25	1.69	5.16	3.76
		Time	450.03	24.82	19.90	2833.5	6.00	5.86
		RMSD	3.71e-1	4.35e-1	1.80e-1	——	5.92e-2	1.37e-2
	2000	rRMSD	3.51e-1	3.63e-1	8.29e-2	——	3.53e-3	3.29e-3
		rTime	40.40	40.65	37.94	——	24.72	4.58
		Time	1255.1	171.01	77.03	——	32.31	17.51

Next we test a number of instances with larger size $n \in \{300, 500, 1000, 2000\}$. For Example 1, the average results were recorded in Table 1. When $R = \sqrt{2}$ under which no dissimilarities were missing because Example 1 was generated in a unit region, PC, ARAP and PREEEDM produced the better RMSD (almost in the order of 10^{-3}). But with the refinement step, all methods led to similar rRMSD. This meant SFSDP and EVEDM benefited a lot from the refinement step. For the computational speed, PREEEDM outperformed others, followed by PC, EVEDM and SFSDP. By contrast, ARAP consumed too much time even for $n = 500$. When $R = 0.2$, the picture was significantly different since there were large amounts of unavailable dissimilarities in Δ. Basically, ADMMSNL, PC and SFSDP failed to localize even with the refinement due to undesirable RMSD and rRMSD (both in the order of 10^{-1}). Clearly, ARAP and PREEEDM produced the best RMSD and rRMSD, and EVEDM got comparable rRMSD but inaccurate RMSD. In terms of the computational speed, EVEDM and PREEEDM were very fast, consuming about 30 seconds to solve problems with $n = 2000$ nodes. By contrast, ARAP still was the slowest, followed by ADMMSNL and PC.

Table 2: Comparisons of six methods for Example 3 with $m = 10, \mathtt{nf} = 0.1$.

	n		ADMMSNL	PC	SFSDP	ARAP	EVEDM	PREEEDM
$R = \sqrt{1.25}$	300	RMSD	4.02e-2	5.33e-3	1.45e-1	1.27e-2	1.62e-1	9.26e-3
		rRMSD	5.12e-3	5.14e-3	5.11e-3	5.12e-3	5.09e-3	5.15e-3
		rTime	3.28	0.66	3.71	1.69	3.94	1.44
		Time	346.98	2.00	6.74	553.87	4.42	1.87
	500	RMSD	––	4.09e-3	1.07e-1	8.50e-3	1.63e-1	7.15e-3
		rRMSD	––	4.03e-3	4.04e-3	4.05e-3	1.02e-1	4.15e-3
		rTime	––	2.68	17.28	7.07	17.39	3.12
		Time	––	7.24	23.44	2556.3	18.89	5.13
	1000	RMSD	––	3.07e-3	1.12e-1	––	1.28e-1	5.05e-3
		rRMSD	––	2.98e-3	3.50e-3	––	4.15e-3	3.15e-3
		rTime	––	10.35	119.79	––	122.12	15.73
		Time	––	43.69	140.66	––	125.46	20.11
	2000	RMSD	––	2.36e-3	1.15e-1	––	1.03e-1	3.75e-3
		rRMSD	––	2.28e-3	7.34e-3	––	7.78e-3	2.26e-3
		rTime	––	13.43	537.70	––	489.30	10.59
		Time	––	238.31	659.71	––	500.72	20.25
$R = 0.1$	300	RMSD	1.81e-1	3.77e-1	8.64e-2	8.19e-2	4.06e-1	3.97e-2
		rRMSD	1.43e-1	1.24e-1	6.69e-2	5.38e-2	1.17e-1	8.21e-3
		rTime	0.27	0.22	0.21	0.21	0.22	0.21
		Time	76.57	1.21	3.24	7.24	3.41	0.32
	500	RMSD	9.73e-2	3.30e-1	5.08e-2	5.77e-2	2.16e-1	3.63e-2
		rRMSD	7.82e-2	1.15e-1	3.48e-2	3.08e-2	9.78e-2	3.63e-3
		rTime	0.67	0.63	0.60	0.58	0.61	0.50
		Time	148.06	3.63	6.41	50.81	2.07	1.85
	1000	RMSD	2.26e-1	3.29e-1	4.80e-2	8.75e-2	2.22e-1	5.01e-2
		rRMSD	1.01e-1	1.21e-1	9.15e-3	4.55e-2	1.02e-1	2.95e-3
		rTime	2.74	2.66	2.67	2.58	2.61	2.60
		Time	353.07	18.01	17.10	842.43	3.22	4.24
	2000	RMSD	1.66e-1	3.29e-1	8.21e-2	––	1.02e-1	5.73e-2
		rRMSD	1.22e-1	1.53e-1	7.10e-2	––	3.64e-2	4.97e-3
		rTime	23.22	23.30	23.06	––	23.12	17.99
		Time	887.30	108.81	62.65	––	26.12	29.89

Now we test those methods for the irregular network in Example 3. The average results were recorded in Table 2. We note that no or large numbers of dissimilarities were missing when $R = \sqrt{1.25}$ and $R = 0.1$ respectively because this example was generated in region $[0,1] \times [0,0.5]$ as presented in Fig. 2. When $R = \sqrt{1.25}$, it can be clearly seen that SFSDP and EVEDM failed to localize before the refinement step due to their large RMSD (in the order of 10^{-1}), whilst the rest four methods succeeded. However, they all achieved a similar rRMSD after the refinement except for EVEDM under the case $n = 500$. Still, PREEEDM ran the fastest and ARAP came the last, (5.13s vs. 2556.3s when $n = 500$). Their performances for the case $R = 0.1$ are quite contrasting. We observed that PREEEDM generated the most accurate RMSD and rRMSD (in the order of 10^{-3}) whilst the results of the rest methods were only in the order of 10^{-2}. Obviously, ADMMSNL, PC and EVEDM failed to localize. Compared with the other four methods, EVEDM and PREEEDM were joint winners in terms of the computational speed, only using 30s when $n = 2000$ (a larger scale network). But we should mention that EVEDM failed to localize.

b) Effect of the number of anchors m. As one would expect, more anchors would lead to more information available, and hence lead to easier localization. In this part, we demonstrate the degree of the effect of the varying numbers of the anchors on the 6 methods. For Example 2, we fix $n = 200, R = 0.2$, nf$= 0.1$ with changing m from $\{5, 10, \cdots, 40\}$. As illustrated in Figure 4, ARAP and PREEEDM were again joint winners in terms of both RMSD and rRMSD. And rRMSD produced by the rest methods declined rapidly as more anchors being added on. Moreover, PREEEDM was the fastest, followed by EVEDM, PC and SFSDP, whilst ADMMSNL and ARAP were quite slow.
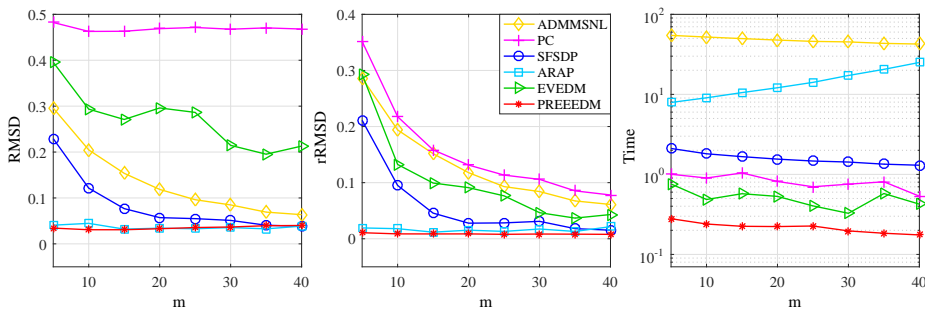
Fig. 4: Average results for Example 2 with $n = 200, R = 0.2$, nf$= 0.1$.

For Example 3 with fixed $n = 500, R = 0.1$, nf$= 0.1$, we test it under $m \in \{10, 30, 50\}$. As depicted in Fig. 5, ARAP and PREEEDM were always capable of capturing the shape of letters 'E', 'D' and 'M' that was similar to Fig. 2. By contrast, SFSDP and EVEDM derived desirable outline of three letters only when $m = 50$, and the localization quality of both ADMMSNL and PC improved along with the increasing m but still with a deformed shape of letter 'M'.

Fig. 5: Localization for Example 3 with $n = 500$, $R = 0.1$, $\texttt{nf} = 0.1$.

Finally we test a number of instances of Example 2 with $n \in \{300, 500, 1000, 2000\}$ and $m \in \{10, 50\}$. The average results were recorded in Tab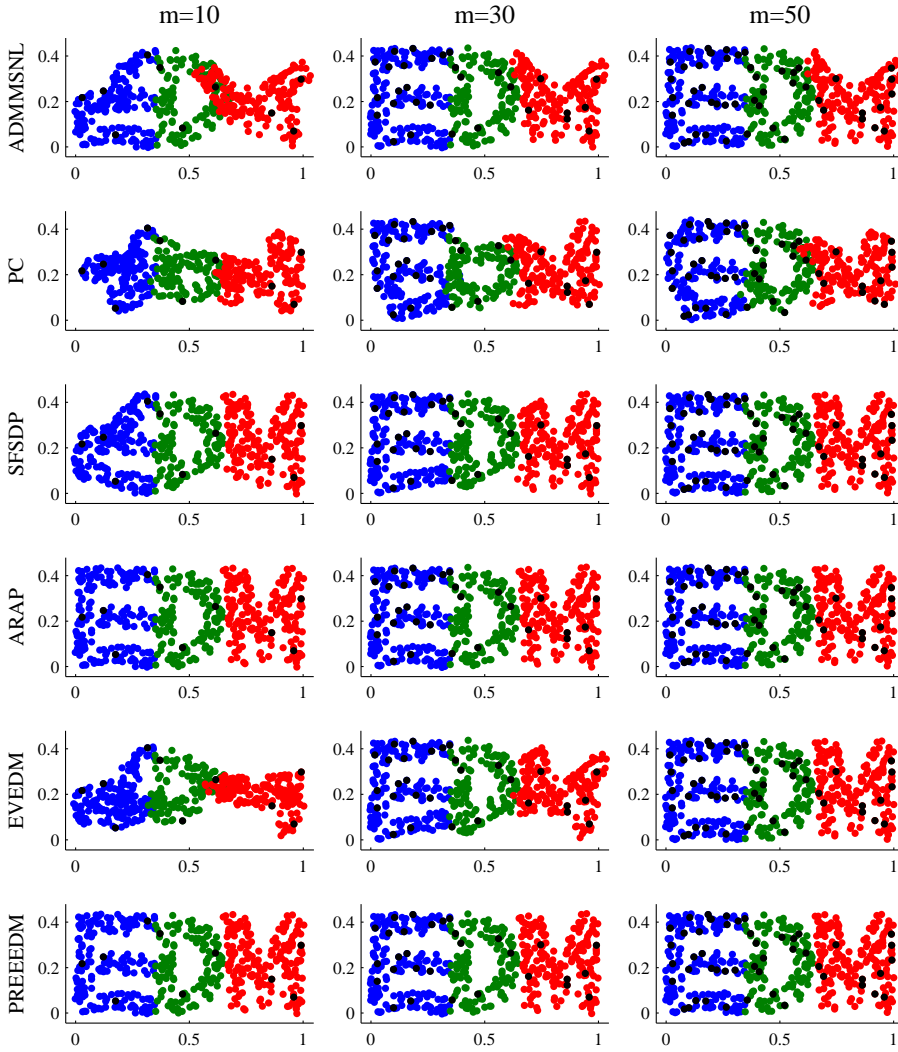le 3. When $m = 10$, $\texttt{ADMMSNL}$ and $\texttt{PC}$ produced undesirable $\texttt{RMSD}$ and $\texttt{rRMSD}$ (both in the order of 10^{-1}). $\texttt{SFSDP}$ benefited greatly from the refinement because it generated relatively inaccurate $\texttt{RMSD}$. By contrast the rest three methods enjoyed the successful localization except for $\texttt{EVEDM}$ under the case $n = 300$. With regard to the computational speed, $\texttt{EVEDM}$ and $\texttt{PREEEDM}$ were the fastest, followed by $\texttt{SFSDP}$, $\texttt{PC}$, $\texttt{ADMMSNL}$ and $\texttt{ARAP}$. When $m = 50$, more information was known, the results were better than before, especially for the methods $\texttt{ADMMSNL}$ and $\texttt{PC}$. But $\texttt{PC}$ still heavily relied on the refinement step to get the satisfactory localization. The rest five methods produced

a satisfactory localization with varying degree of accuracy. It is encouraging to see that PREEEDM produced the most accurate rRMSD for all cases. The comparison of the computational speed is similar to the case of $m = 10$. We repeated the test for Example 3 and the average results were recorded in Table 4, where we observed a similar performance of the six methods as for Example 2. We omit the details.

Table 3: Comparisons of six methods for Example 2 with $R = 0.2, \mathtt{nf} = 0.1$.

	n		ADMMSNL	PC	SFSDP	ARAP	EVEDM	PREEEDM
$m = 10$	300	RMSD	2.56e-1	4.59e-1	1.34e-1	2.60e-2	2.72e-1	3.99e-2
		rRMSD	2.49e-1	2.43e-1	7.19e-2	6.71e-3	1.44e-1	6.69e-3
		rTime	0.40	0.43	0.36	0.26	0.39	0.28
		Time	81.62	2.02	3.18	24.92	0.47	0.40
	500	RMSD	1.86e-1	4.41e-1	9.70e-2	2.42e-2	8.62e-2	3.29e-2
		rRMSD	1.82e-1	2.07e-1	4.99e-2	5.07e-3	5.05e-3	5.07e-3
		rTime	0.81	1.30	0.93	0.69	0.84	0.64
		Time	163.55	4.70	6.67	170.82	1.04	1.02
	1000	RMSD	1.82e-1	4.39e-1	9.93e-2	2.71e-2	6.88e-2	3.95e-2
		rRMSD	1.60e-1	1.96e-1	2.92e-2	3.21e-3	3.20e-3	3.63e-3
		rTime	4.79	5.53	4.38	3.90	4.66	3.71
		Time	441.08	24.70	18.64	2861.9	5.47	5.88
	2000	RMSD	2.17e-1	4.39e-1	1.30e-1	——	6.08e-2	5.03e-2
		rRMSD	1.87e-1	2.54e-1	6.88e-2	——	2.64e-3	2.82e-3
		rTime	39.22	39.32	36.29	——	33.85	14.43
		Time	1251.07	170.55	75.29	——	37.33	28.95
$m = 50$	300	RMSD	3.19e-2	4.49e-1	3.09e-2	5.30e-2	1.09e-1	5.07e-2
		rRMSD	3.10e-2	4.39e-2	1.13e-2	1.26e-2	1.84e-2	5.78e-3
		rTime	0.12	0.20	0.09	0.09	0.11	0.09
		Time	74.71	1.44	2.41	48.83	0.22	0.25
	500	RMSD	2.80e-2	4.60e-1	3.54e-2	4.39e-2	5.10e-2	6.09e-2
		rRMSD	2.68e-2	4.93e-2	6.77e-3	4.42e-3	5.61e-3	4.42e-3
		rTime	0.24	0.50	0.21	0.21	0.19	0.19
		Time	144.93	4.25	4.67	232.14	0.46	0.72
	1000	RMSD	1.91e-2	4.57e-1	3.21e-2	2.27e-2	5.06e-2	5.99e-2
		rRMSD	1.27e-2	3.75e-2	4.76e-3	2.94e-3	2.94e-3	2.94e-3
		rTime	1.05	2.52	1.10	1.05	1.01	1.12
		Time	406.88	20.29	12.48	3150.6	1.86	4.02
	2000	RMSD	2.17e-2	4.47e-1	3.63e-2	——	5.16e-2	4.72e-2
		rRMSD	6.13e-3	2.78e-2	3.52e-3	——	2.06e-3	2.06e-3
		rTime	11.89	25.95	10.43	——	8.80	7.71
		Time	1171.22	156.45	40.45	——	11.15	22.53

c) Effect of the noise factor nf. To see the dependence of the performance of each method on the noise factor, we first test Example 3 with fixing $n = 200, m = 10, R = 0.3$ and varying the noise factor $\mathtt{nf} \in \{0.1, 0.2, \cdots, 0.7\}$. As shown in Fig. 6, in terms of RMSD it can be seen that ARAP got the smallest ones, whilst EVEDM and PC obtained the worst ones. The line of ADMMSNL dropped down from $0.1 \leq \mathtt{nf} \leq 0.3$ and then ascended. By contrast the line of PREEEDM reached the peak at $\mathtt{nf} = 0.3$ but declined afterwards and gradually approached to RMSD of ARAP. However, after the refinement step, ARAP, SFSDP and PREEEDM all derived a similar rRMSD while the other three methods produced undesirable ones. Apparently, EVEDM was indeed the fastest (yet with the worst rRMSD), followed by PC, SFSDP and PREEEDM. Again, ARAP and ADMMSNL were quite slow.

Table 4: Comparisons of six methods for Example 3 with $R = 0.1, \mathtt{nf} = 0.1$.

	n		ADMMSNL	PC	SFSDP	ARAP	EVEDM	PREEEDM
$m = 10$	300	RMSD	1.80e-1	3.77e-1	8.86e-2	7.97e-2	3.88e-1	4.05e-2
		rRMSD	1.48e-1	1.24e-1	6.24e-2	4.51e-2	1.19e-1	6.25e-3
		rTime	0.28	0.22	0.21	0.22	0.23	0.21
		Time	76.83	1.12	3.00	7.22	5.92	0.41
	500	RMSD	9.71e-2	3.30e-1	4.97e-2	5.97e-2	2.10e-1	3.81e-2
		rRMSD	8.07e-2	9.98e-2	3.21e-2	3.38e-2	1.04e-1	3.91e-3
		rTime	0.68	0.59	0.60	0.59	0.59	0.47
		Time	142.20	3.37	6.35	48.98	2.10	0.98
	1000	RMSD	2.30e-1	3.29e-1	4.98e-2	8.86e-2	2.24e-1	4.93e-2
		rRMSD	1.02e-1	1.18e-1	2.33e-2	4.53e-2	1.07e-1	2.37e-3
		rTime	2.92	2.84	2.82	2.80	2.85	2.84
		Time	354.77	18.59	17.43	838.48	3.85	4.55
	2000	RMSD	1.66e-1	3.29e-1	7.96e-2	$--$	1.03e-1	5.72e-2
		rRMSD	1.22e-1	1.52e-1	6.92e-2	$--$	4.25e-2	4.89e-3
		rTime	23.24	23.17	23.08	$--$	23.05	13.07
		Time	882.40	98.20	66.58	$--$	26.21	24.17
$m = 50$	300	RMSD	2.24e-2	3.34e-1	1.72e-2	4.04e-2	2.22e-1	3.35e-2
		rRMSD	2.13e-2	2.44e-2	8.36e-3	1.19e-2	2.11e-2	4.34e-3
		rTime	0.22	0.21	0.11	0.13	0.22	0.14
		Time	69.59	0.55	2.30	26.37	0.30	0.29
	500	RMSD	2.53e-2	3.41e-1	2.50e-2	4.95e-2	6.14e-2	4.18e-2
		rRMSD	2.46e-2	3.67e-2	6.64e-3	4.89e-3	2.97e-3	2.96e-3
		rTime	0.34	0.58	0.42	0.38	0.43	0.37
		Time	130.58	2.96	5.07	83.65	0.60	0.79
	1000	RMSD	1.97e-2	3.30e-1	1.94e-2	4.82e-2	5.60e-2	4.90e-2
		rRMSD	1.89e-2	3.07e-2	1.95e-3	3.50e-3	1.96e-3	1.96e-3
		rTime	1.02	2.78	1.04	1.49	1.36	1.23
		Time	314.30	14.31	12.87	947.29	1.97	3.48
	2000	RMSD	4.64e-3	3.28e-1	2.10e-2	$--$	6.30e-2	5.72e-2
		rRMSD	1.32e-3	3.01e-2	1.32e-3	$--$	1.32e-3	1.32e-3
		rTime	14.59	23.23	13.03	$--$	13.87	8.28
		Time	811.23	99.02	44.12	$--$	15.99	19.45
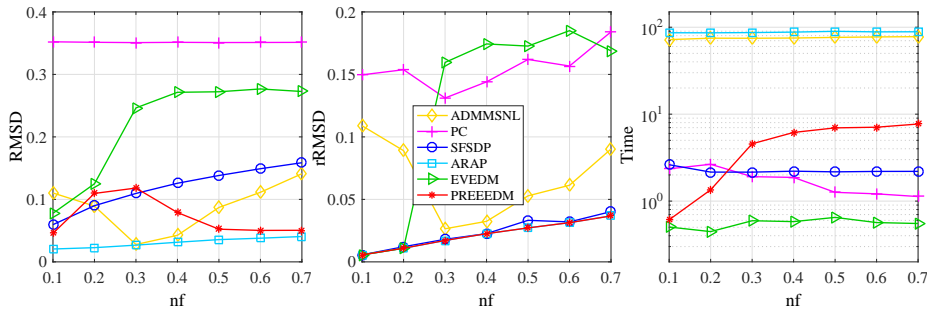
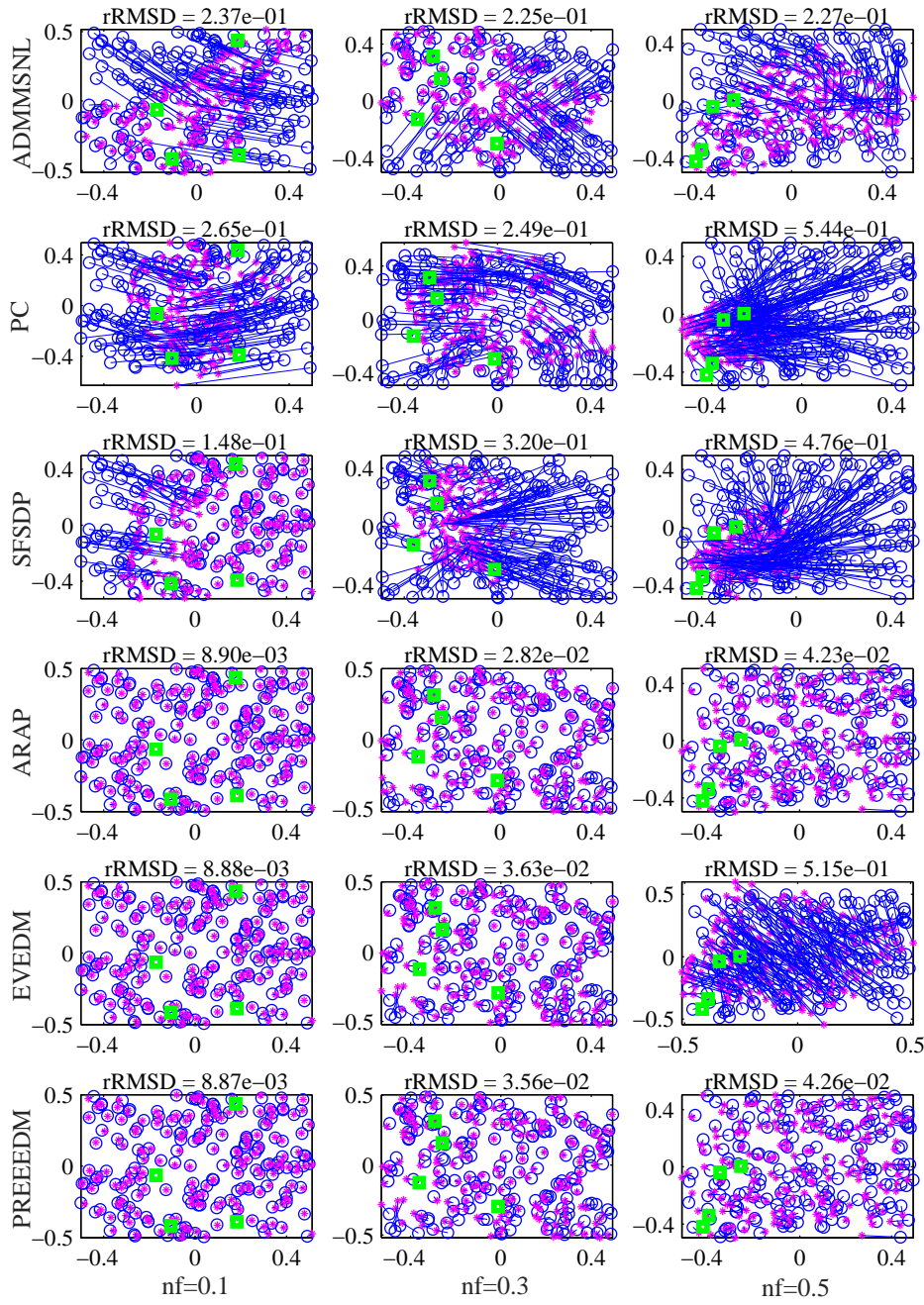Fig. 6: Average results for Example 3 with $n = 200, m = 10, R = 0.3$.

Fig. 7: Localization for Example 2 with $n = 200, m = 4, R = 0.3$.

Next, we test Example 2 with a moderate size (for the visualization purpose in Fig. 7) $n = 200, m = 4$ and $R = 0.3$ and varying $\mathtt{nf} \in \{0.1, 0.3, 0.5\}$. The

actual embedding by each method was shown in Fig. 7, where the four anchors were plotted in green square and $\widehat{\mathbf{x}}_i$ in pink points were jointed to its ground truth location (blue circle). It can be clearly seen that ARAP and PREEEDM were quite robust to the noise factor since their localization matched the ground truth well. EVEDM failed to locate when nf = 0.5. By contrast, SFSDP generated worse results when nf got bigger, and ADMMSNL and PC failed to localize for all cases.

Finally, we test Example 1 with larger sizes $n \in \{300, 500, 1000, 2000\}$ and fixed $m = 4, R = 0.3$. The average results were recorded in Table 5. When nf = 0.1, ADMMSNL and PC failed to render accurate embedding. Compared with ARAP, EVEDM and PREEEDM, SFSDP generated lager RMSD and rRMSD. Again, EVEDM and PREEEDM ran faster than ARAP. When nf = 0.7, the results were different. ARAP and PREEEDM were still able to produce high-quality RMSD and rRMSD. However, the former took extremely long time (16617 vs. 83 seconds). By contrast, ADMMSNL and PC again failed to reconstruct the network. Furthermore, EVEDM got large RMSD but comparable rRMSD when $n \le 1000$, but it failed when $n = 2000$.

Table 5: Comparisons of six methods for Example 1 with $m = 4, R = 0.3$.

	n		ADMMSNL	PC	SFSDP	ARAP	EVEDM	PREEEDM
nf = 0.1	300	RMSD	3.16e-1	4.46e-1	1.74e-1	1.03e-2	6.58e-2	1.64e-2
		rRMSD	2.84e-1	3.10e-1	9.63e-2	6.62e-3	6.55e-3	6.57e-3
		rTime	0.75	0.71	0.62	0.31	0.43	0.34
		Time	101.07	3.09	4.39	117.33	0.55	0.57
	500	RMSD	2.96e-1	4.02e-1	1.59e-1	6.73e-3	5.25e-2	1.25e-2
		rRMSD	2.14e-1	2.81e-1	6.05e-2	4.59e-3	4.64e-3	4.73e-3
		rTime	1.68	1.74	1.50	0.50	1.03	0.81
		Time	182.09	9.10	6.16	769.39	1.32	1.48
	1000	RMSD	3.47e-1	4.77e-1	1.83e-1	5.35e-3	5.57e-2	1.13e-2
		rRMSD	2.71e-1	2.52e-1	5.52e-2	3.63e-3	3.65e-3	3.49e-3
		rTime	14.89	15.11	12.00	1.97	10.32	5.22
		Time	601.92	56.65	24.49	15686.4	11.63	10.03
	2000	RMSD	——	4.47e-1	1.81e-1	——	5.53e-2	1.16e-2
		rRMSD	——	4.25e-1	2.21e-2	——	3.32e-3	3.12e-3
		rTime	——	82.17	82.35	——	45.12	5.85
		Time	——	470.32	122.45	——	49.18	34.68
nf = 0.7	300	RMSD	2.80e-1	4.36e-1	3.27e-1	6.70e-2	2.08e-1	5.04e-2
		rRMSD	2.31e-1	3.60e-1	2.47e-1	5.48e-2	6.10e-2	4.92e-2
		rTime	0.75	0.83	0.83	0.29	0.47	0.38
		Time	107.48	1.74	83.73	123.18	0.59	7.49
	500	RMSD	2.64e-1	4.53e-1	——	4.24e-2	1.76e-1	3.73e-2
		rRMSD	1.94e-1	3.59e-1	——	3.52e-2	3.47e-2	3.23e-2
		rTime	1.66	1.88	——	0.47	0.87	0.67
		Time	177.24	5.13	——	844.74	1.31	20.15
	1000	RMSD	2.21e-1	4.52e-1	——	2.84e-2	1.45e-1	2.79e-2
		rRMSD	9.69e-2	3.26e-1	——	2.47e-2	2.93e-2	2.40e-2
		rTime	9.83	15.69	——	1.41	7.78	2.54
		Time	599.30	41.55	——	16617.1	9.16	83.64
	2000	RMSD	——	4.51e-1	——	——	2.26e-1	2.13e-2
		rRMSD	——	3.35e-1	——	——	1.23e-1	1.52e-2
		rTime	——	92.45	——	——	58.25	3.79
		Time	——	274.90	——	——	62.52	303.43

6.4.2 Comparison on MC

As we mentioned before, the current implementations of `ADMMSNL`, `ARAP` do not support the embedding for $r \geq 3$ and thus are removed in the following comparison, where the method `PPAS` will be added. The main reason for adding `PPAS` is that it is particularly suitable and credible for the MC problems [24, 25].

d) Test on Example 4. To see the performance of each method on this problem, we first test it with fixing $s = 6$ ($n = 6^3$), `nf` = 0.1 but varying $R \in \{36, 38, \cdots, 48\}$. We note that the percentage of available dissimilarities increased from 32.47% to 39.87% with R increasing from 36 to 48, making the problem become 'easier' for conformation. The Average results were recorded in Fig. 8. Clearly, `PREEEDM` and `PPAS` outperformed the other three methods in terms of `RMSD` and `rRMSD`. The former generated the best `RMSD` when $R \geq 42$ while the latter got the best `RMSD` when $R \leq 42$, but they both obtained similar `rRMSD`. As for the computational speed, `PREEEDM` ran far more faster than `PPAS`. By contrast, the other three methods failed to produce accurate embeddings due to the worse `RMSD` and `rRMSD` obtained. Notice that the refinement would not always make the final results better. For instance, `rRMSD` yielded by `SFSDP` was bigger than `RMSD` for each s.
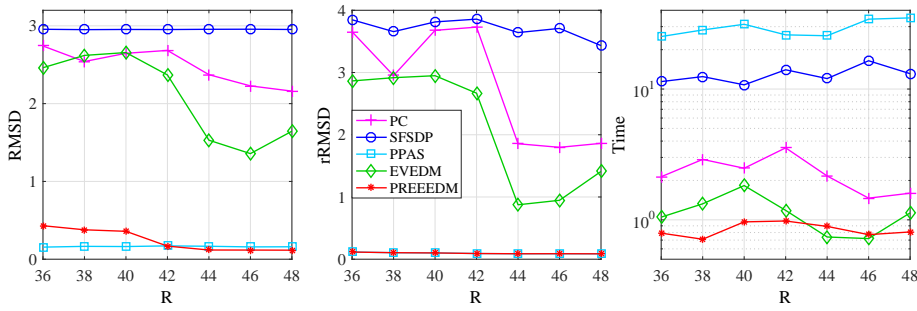

Fig. 8: Average results for Example 4 with $s = 6, \mathtt{nf} = 0.1$.
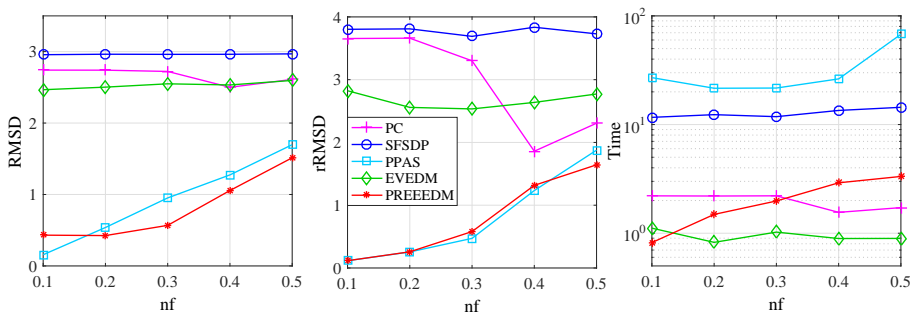

Fig. 9: Average results for Example 4 with $s = 6, R = s^2$.

We then test the example with fixing $s = 6$ ($n = 6^3$), $R = s^2$ and varying $\mathtt{nf} \in \{0.1, 0.2, \cdots, 0.5\}$. As illustrated in Fig. 9, in terms of $\mathtt{RMSD}$ and $\mathtt{rRMSD}$, it can be clearly seen that $\mathtt{PREEEDM}$ and $\mathtt{PPAS}$ were the joint winners. In particular, our method rendered the best $\mathtt{RMSD}$ when $\mathtt{nf} \geq 0.2$ and also ran much faster than $\mathtt{PPAS}$. Obviously, the other three methods again failed to obtain desirable $\mathtt{RMSD}$ and $\mathtt{rRMSD}$ irrelevant of the time they used.

Finally, for larger size problems with $n = s^3$ and $s \in \{7, 8, \ldots, 13\}$, the average results were presented in Fig. 10, where we omitted the results by $\mathtt{PPAS}$ for $s > 10$ because it took too much time to terminate. It is worth mentioning that the percentage of the available dissimilarities over all elements of Δ decreases from 26.78% to 14.83% when s increasing from 7 to 13, making the problems more and more challenging. Clearly $\mathtt{PC}$, $\mathtt{SFSDP}$ and $\mathtt{EVEDM}$ failed to locate all atoms in $\Re^3$. $\mathtt{PPAS}$ rendered the most accurate $\mathtt{RMSD}$ when $s \leq 10$ whilst $\mathtt{PREEEDM}$ achieved the most accurate $\mathtt{RMSD}$ when $s > 10$ and the most accurate $\mathtt{rRMSD}$ for all cases. Equally important for $\mathtt{PREEEDM}$ is that it spent less than 50 seconds for all tested cases, while $\mathtt{PPAS}$ took much more time to terminate (e.g., consuming over 2000 seconds when $s \geq 10$).
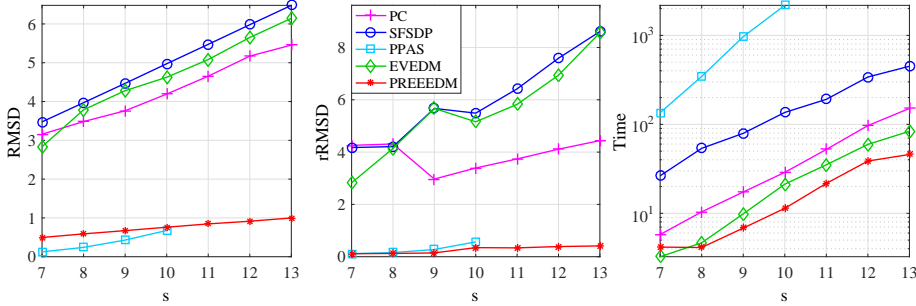

Fig. 10: Average results for Example 4 with $n = s^3, R = s^2, \mathtt{nf} = 0.1$.

e) Test on Example 5. For the 12 collected real data, we fixed $R = 6, c = 50\%$ and $\mathtt{nf} = 0.1$. The generated embeddings by the five methods for the three molecules $\mathtt{1GM2}$, $\mathtt{1AU6}$ and $\mathtt{1LFB}$ were shown in Fig. 11, where the true and estimated positions of the atoms were plotted by blue circles and pink stars respectively. Each pink star was linked to its corresponding blue circle by a pink line. For these three data, $\mathtt{PREEEDM}$ and $\mathtt{PPAS}$ almost conformed the shape of the original data. Clearly, the other three methods failed to conform. The complete numerical results for the 12 problems were reported in Table 6. It can be clearly seen that $\mathtt{PREEEDM}$ and $\mathtt{PPAS}$ performed significantly better in terms of the $\mathtt{RMSD}$ and $\mathtt{rRMSD}$ than the other methods. What is more impressive is that $\mathtt{PREEEDM}$ only used a small fraction of the time by $\mathtt{PPAS}$, which in general took relatively long time to terminate. For example, $\mathtt{PREEEDM}$ only used 22.64 seconds for $\mathtt{2CLJ}$, which is a very large data set with $n = 4189$. In contrast, we had to omit the result of $\mathtt{PPAS}$ for this instance (as well as to omit for other tested instances, and the missed results were indicated as "$--$" in Table 6) because it took too long to terminate.

(a) PC:rRMSD=8.39   (b) PC:rRMSD=10.7   (c) PC:rRMSD=13.7

(d) SFSDP:rRMSD=7.86   (e) SFSDP:rRMSD=9.55   (f) SFSDP:rRMSD=14.2

(g) PPAS:rRMSD=0.267   (h) PPAS:rRMSD=0.173   (i) PPAS:rRMSD=0.680

(j) EVEDM:rRMSD=9.75   (k) EVEDM:rRMSD=10.0   (l) EVEDM:rRMSD=14.2

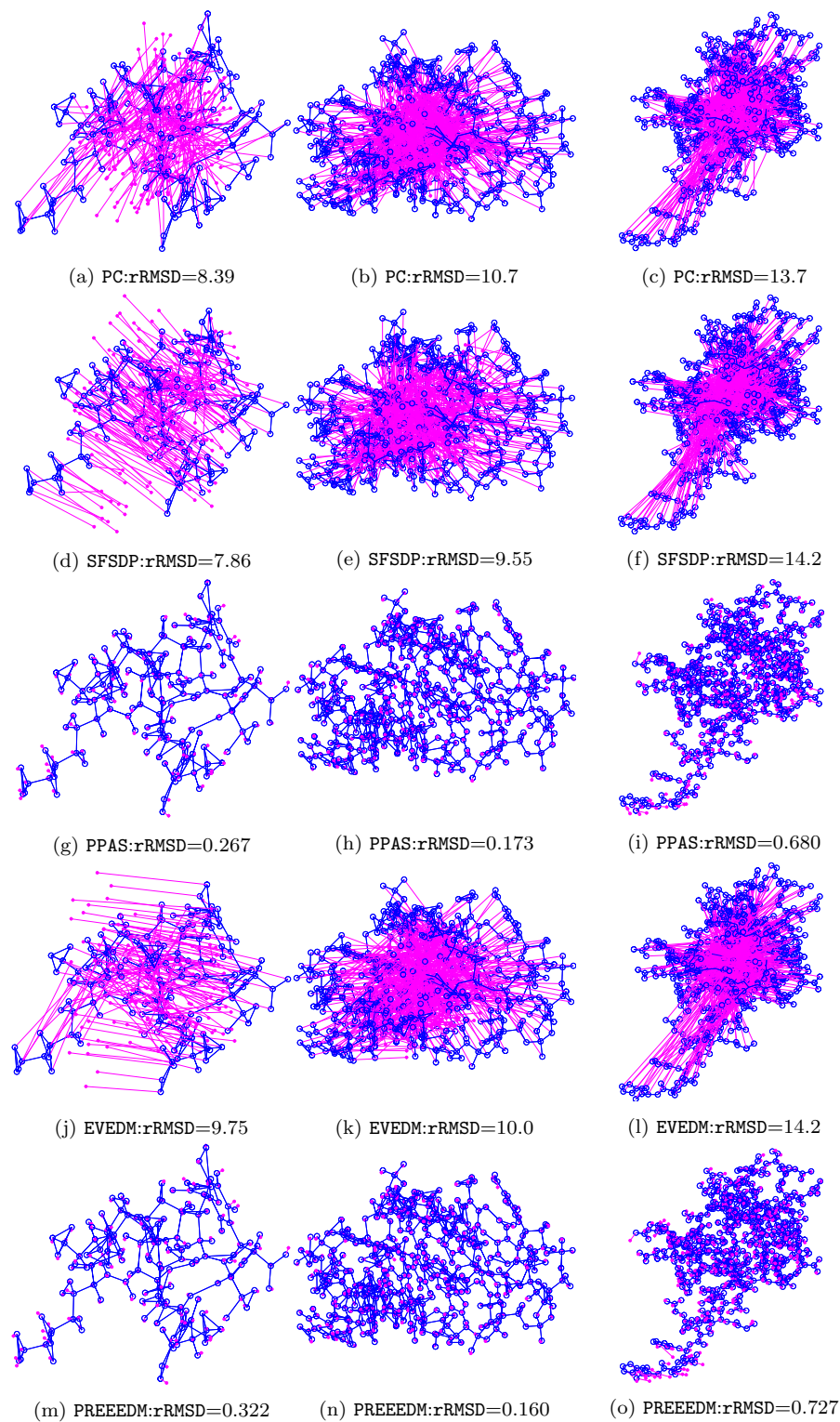(m) PREEEDM:rRMSD=0.322   (n) PREEEDM:rRMSD=0.160   (o) PREEEDM:rRMSD=0.727

Fig. 11: Molecular conformation by PC, SFSDP, PPAS, EVEDM and PREEEDM. Left: 1GM2 ($n = 166$); Middle: 1AU6 ($n = 506$); Right: 1LFB ($n = 641$).

Table 6: Comparisons of the five methods for Example 5.

		PC	SFSDP	PPAS	EVEDM	PREEEDM
1GM2 $n = 166$	RMSD	6.60e+0	6.65e+0	4.07e-1	6.51e+0	9.09e-1
	rRMSD	7.07e+0	6.92e+0	2.65e-1	7.41e+0	3.51e-1
	rTime	0.17	0.18	0.22	0.18	0.16
	Time	0.98	4.84	15.43	0.98	0.27
304D $n = 237$	RMSD	1.03e+1	1.03e+1	2.89e+0	1.02e+1	3.61e+0
	rRMSD	1.07e+1	1.08e+1	1.43e+0	1.08e+1	2.50e+0
	rTime	0.16	0.16	0.55	0.16	0.15
	Time	1.07	7.76	36.44	1.36	0.23
1PBM $n = 388$	RMSD	8.45e+0	8.47e+0	5.29e-1	8.35e+0	1.23e+0
	rRMSD	9.13e+0	8.91e+0	2.01e-1	9.28e+0	2.11e-1
	rTime	0.51	0.49	0.53	0.49	0.32
	Time	2.84	28.64	112.82	1.45	0.54
2MSJ $n = 480$	RMSD	1.06e+1	1.06e+1	5.40e-1	1.05e+1	9.15e-1
	rRMSD	1.12e+1	1.11e+1	2.99e-1	1.10e+1	3.34e-1
	rTime	0.40	0.39	0.54	0.39	0.32
	Time	2.32	118.60	196.12	1.47	0.59
1AU6 $n = 506$	RMSD	9.30e+0	9.31e+0	4.02e-1	9.20e+0	6.74e-1
	rRMSD	9.99e+0	9.83e+0	1.68e-1	9.69e+0	1.63e-1
	rTime	0.70	0.68	0.30	0.69	0.35
	Time	4.12	47.68	262.28	1.47	0.70
1LFB $n = 641$	RMSD	1.34e+1	1.34e+1	1.56e+0	1.33e+1	1.57e+0
	rRMSD	1.39e+1	1.35e+1	5.41e-1	1.37e+1	7.38e-1
	rTime	0.49	0.49	1.63	0.48	0.37
	Time	2.93	132.96	956.44	1.64	0.79
104D $n = 766$	RMSD	1.23e+1	1.23e+1	4.30e+0	1.22e+1	3.27e+0
	rRMSD	1.27e+1	1.27e+1	2.02e+0	1.26e+1	1.26e+0
	rTime	0.89	0.86	3.40	0.87	0.61
	Time	5.04	72.16	2024.51	1.47	1.40
1PHT $n = 814$	RMSD	1.23e+1	1.23e+1	1.70e+0	1.23e+1	1.58e+0
	rRMSD	1.29e+1	1.26e+1	9.16e-1	1.26e+1	9.85e-1
	rTime	0.74	0.74	2.57	0.74	0.48
	Time	4.86	411.14	4726.96	1.71	1.25
1POA $n = 914$	RMSD	1.42e+1	1.42e+1	1.39e+0	1.41e+1	1.48e+0
	rRMSD	1.45e+1	1.46e+1	3.27e-1	1.46e+1	4.51e-1
	rTime	0.58	0.55	1.34	0.55	0.52
	Time	5.03	587.14	1623.43	1.99	1.45
1AX8 $n = 1003$	RMSD	1.43e+1	1.43e+1	−−	1.43e+1	1.23e+0
	rRMSD	1.47e+1	1.45e+1	−−	1.44e+1	5.01e-1
	rTime	0.62	0.58	−−	0.59	0.34
	Time	5.78	1404.53	−−	1.54	1.49
1RGS $n = 2015$	RMSD	2.02e+1	−−	−−	2.02e+1	1.99e+0
	rRMSD	2.05e+1	−−	−−	2.06e+1	6.76e-1
	rTime	1.33	−−	−−	1.25	0.94
	Time	16.08	−−	−−	3.69	5.71
2CLJ $n = 4189$	RMSD	2.27e+1	−−	−−	2.27e+1	1.54e+0
	rRMSD	2.30e+1	−−	−−	2.29e+1	6.50e-1
	rTime	4.46	−−	−−	3.82	2.35
	Time	43.10	−−	−−	378.35	22.64

7 Conclusion

The purpose of this paper is to develop an efficient method for one of the most challenging distance embedding problems in a low-dimensional space, which have been widely studied under the framework of multi-dimensional scaling. The problem employs ℓ_1 norm to quantify the embedding errors. Hence, the resulting model (3) appears to be robust to outliers and is referred to as the robust Euclidean embedding (REE) model.

To the best knowledge of the authors, the only viable method, whose matlab code is also publicly available for REE is the PlaceCenter (PC) algorithm proposed in [1]. Our extensive numerical results on the SNL and MC test problems convincingly demonstrated that the proposed `PREEEDM` method outperform `PC` in terms of both the embedding quality and the `CPU` time. Moreover, `PREEEDM` is also comparable to several state-of-the-art methods for other embedding models in terms of the embedding quality, but is far more efficient in terms of the `CPU` time. The advantage becomes even more superior as the size of the problem gets bigger.

The novelty of the proposed `PREEEDM` lies with its creative use of the Euclidean distance matrix and a computationally efficient majorization technique to derive its subproblem, which has a closed-form solution closely related to the positive root of the classical depressed cubic equation. Furthermore, a great deal of effort has been devoted to its convergence analysis, which well justifies the numerical performance of `PREEEDM`. We feel that `PREEEDM` will become a very competitive embedding method in the field of SNL and MC and expect its wide use in other visualization problems.

References

1. A. Agarwal, J.M. Phillips and S. Venkatasubramanian, Universal multi-dimensional scaling, In Proceedings of the 16th ACM SIGKDD international conference on Knowledge discovery and data mining, pp. 1149-1158, ACM, 2010.
2. LTH AN AND PD TAO, *Large-scale molecular optimization from distance matrices by a dc optimization approach*, SIAM J. Optim. 14 (2003), pp. 77–114.
3. S. BAI AND H.-D. QI, *Tackling the flip ambiguity in wireless sensor network localization and beyond*, Digital Signal Process., 55 (2016), pp. 85-97.
4. H.M. Berman, J. Westbrook, Z. Feng, G. Gillilan, T.N. Bhat, H. Weissig, I.N. Shindyalov and P.E. Bourne, "The protein data bank", Nucleic Acids Res. 28, pp. 235242, 2000.
5. P. BISWAS, T.-C. LIANG, K.-C. TOH, T.-C. WANG AND Y. YE, *Semidefinite programming approaches for sensor network localization with noisy distance measurements*, IEEE Trans. Auto. Sci. Eng., 3, pp. 360-371, 2006.
6. I. BORG AND P.J.F. GROENEN, *Modern Multidimensional Scaling: Theory and Applications*, 2nd Ed., Springer Series in Statistics, Springer, 2005.
7. D.M. BURTON, *The History of Mathematics* (7th Eds), MaGraw-Hill, 2011.
8. L. CAYTON AND S. DASGUPTA *Robust Euclidean embedding*, Proceedings of the 23rd International Conference on Machine Learning, Pittsburgh, PA 2006, pp. 169–176.
9. Y.Q. CHEN, N.H. XIU AND D.T. PENG, *Global solutions of non-Lipschitz S_2S_p minimization over the positive semidefinite cone*, Optimization Letters, 8 (2014), pp. 2053-2064.

10. T.F. Cox and M.A.A. Cox, *Multidimensional Scaling*, 2nd Ed, Chapman and Hall/CRC, 2001.

11. C. Ding and H.-D. Qi, *Convex optimization learning of faithful Euclidean distance representations in nonlinear dimensionality reduction*, Math. Program., 164 (2017), pp. 341-381.

12. D. Drusvyatskiy, N. Krislock, Y.L. Voronin and H. Wolkowicz, *Noisy Euclidean distance realization: robust facial reduction and the Pareto frontier,* SIAM Journal on Optimization, 27(4), 2301-2331, 2017.

13. J. de Leeuw, *Applications of Convex Analysis to Multidimensional Scaling*, In J Barra, F Brodeau, G Romier, B van Cutsem (eds.), *Recent Developments in Statistics*, pp. 133–145. North Holland Publishing Company, Amsterdam, The Netherlands, 1977.

14. J. de Leeuw and P. Mair, *Multidimensional scaling using majorization: Smacof in R*, J. Stat. Software, 31, pp. 1-30, 2009.

15. P. Biswas and Y. Ye, *Semidefinite programming for ad hoc wireless sensor network localization*, in *Proceedings of the 3rd IPSN*, Berkeley, CA, pp. 46-54, 2004.

16. D. Drusvyatskiy, N. Krislock, Y.-L. Voronin and H. Wolkowicz, *Noisy Euclidean distance realization: Robust facial reduction and the Pareto frontier*, SIAM J. Optim., 27(2017), 2301–2331.

17. S.L. France and J.D. Carroll, *Two-way multidimensional scaling: a review*, IEEE Trans. Syst. Man, and Cyber. – Part C, 41 (2011), pp. 644-661.

18. Y. Gao, *Structured Low Rank Matrix Optimization Problems: a Penalty Approach*, PhD Thesis, National University of Singapore, 2010.

19. N. Gaffke and R. Mathar, *A cyclic projection algorithm via duality*, Metrika, 36 (1989), pp. 29-54.

20. W. Glunt, T.L. Hayden, S. Hong and J. Wells, *An alternating projection algorithm for computing the nearest Euclidean distance matrix*, SIAM J. Matrix Anal. Appl., 11 (1990), pp. 589-600.

21. W. Glunt, T.L. Hayden and R. Raydan, *Molecular conformations from distance matrices*, J. Comput. Chemistry, 14 (1993), pp. 114-120.

22. J.C. Gower 1966, *Some distance properties of latent root and vector methods used in multivariate analysis*, Biometrika 53 (1966), pp. 325–338.

23. W.J. Heiser, *Multidimensional scaling with least absolute residuals*, in Proceedings of the First Conference of the International Federation of Classification Societies (IFCS), Aachen, Germany, June 1987, pp. 455-462.

24. K.F. Jiang, D.F Sun and K.C. Toh, *Solving nuclear norm regularized and semidefinite matrix least squares problems with linear equality constraints*, Discrete Geometry and Optimization, Springer International Publishing, pp. 133-162, 2013.

25. K.F. Jiang, D.F. Sun and K.-C. Toh, *A partial proximal point algorithm for nuclear norm regularized matrix least squares problems*, Math. Programming Comput., 6 (2014), 281–325.

26. C. Kanzow and H.-D. Qi, *A QP-free constrained Newton-type method for variational inequality problems*, Math. Prog., 85 (1999), pp. 81-106.

27. S. Kim, M. Kojima, H. Waki and M. Yamashita, *Algorithm 920: SFSDP: A sparse version of full semidefinite programming relaxation for sensor network localization problems*, ACM Trans. Math. Softw., 38(4), pp. 27:1-27:19, 2012.

28. S. Korkmaz and A.J. Van der Veen, *Robust localization in sensor networks with iterative majorization techniques*, ICASSP, 2009, pp. 2049-2052.

29. J.B. Kruskal, *Nonmetric multidimensional scaling: a numerical method*, Psychometrika, 29 (1964), pp. 115-129.

30. F.D. Mandanas and C.L. Kotropoulos, *Robust multidimensional scaling using a maximum correntropy criterion*, IEEE Trans. Signal Process., 65 (2017), pp. 919–932.

31. C.A. Micchelli, *Interpolation of scattered data: distance matrices and conditionally positive definite functinos*, Constr. Approx., 2 (1986), pp. 11-22.

32. J.J. More and Z. Wu, Global continuation for distance geometry problems, SIAM J. Optim., 7, pp. 814836, 1997.

33. G. Nocedal and S.J. Wright, *Numerical Optimization* (2nd Eds), Springer, 2006.

34. P. Oğuz-Ekim, J.P. Gomes, J. Xavier and P. Oliveira, *Robust localization of nodes and time-recursive tracking in sensor networks using noisy range measurements*, IEEE Trans. Signal Process., 59 (2011), pp. 3930-3942.

35. D.T Peng, N.H. Xiu and J. Yu, $S_{1/2}$ *regularization methods and fixed point algorithms for affine rank minimization problems*, Comput. Optim. Appl., 67 (2017), pp. 543–569.

36. N. Piovesan and T. Erseghe, *Cooperative localization in WSNs: a hybrid convex/non-convex solution*, IEEE Trans. Signal and Information Processing over Networks, DOI 10.1109/TSIPN.2016.2639442 (IEEE early access article, 2016).

37. T.K. Pong, *Edge-based semidefinite programming relaxation of sensor network localization with lower bound constraints*, Comput Optim Appl., 53, pp. 23-44, 2012.

38. H.-D. Qi, *A semismooth Newton method for the nearest Euclidean distance matrix problem*, SIAM J. Matrix Anal. Appl. 34 (2013), pp. 67-93.

39. H.-D. Qi and X.M. Yuan, *Computing the nearest Euclidean distance matrix with low embedding dimensions*, Math. Prog., 147 (2014), pp. 351-389.

40. H.-D. Qi, N.H. Xiu, and X.M. Yuan, *A Lagrangian dual approach to the single source localization problem*, IEEE Trans. Signal Process., 61, pp. 3815-3826, 2013.

41. R.T. Rockafella and R. J-B Wets, Variational Analysis (3rd Eds), Springer, 2009.

42. I.J. Schoenberg, *Remarks to Maurice Frechet's article Sur la definition axiomatque d'une classe d'espaces vectoriels distancies applicbles vectoriellement sur l'espace de Hilbet*, Ann. Math., 36 (1935), pp. 724-732.

43. Y. Shang, W. Ruml, Y. Zhang and M.P.J. Fromherz, *Localization from mere connectivity*, in: *Proceedings of the 4th ACM International Symposium on Mobile Ad Hoc Networking & Computing*, MobiHoc 03, ACM, New York, NY, USA, pp. 201-212, 2003.

44. C. Soares, J. Xavier and J. Gomes, *Simple and fast convex relaxation method for cooperative localization in sensor networks using range measurements*, IEEE Trans. Signal Process., 63(17), pp. 4532-4543, 2015.

45. Y. Sun, P. Babu and D.P. Palomar, *Majorization-minimization algorithms in signal processing, communications, and machine learning*, IEEE Trans. Signal Process., 65 (2017), pp. 794-816.

46. J.B. Tenenbaum, V. de Silva and J.C. Langford, *A global geometric framework for nonlinear dimensionality reduction*, Science, 290 (2000), pp. 2319-2323.

47. K.C. Toh, *An inexact path-following algorithm for convex quadratic SDP*, Math. Prog., 112 (2008), pp. 221254.

48. W.S. Torgerson, *Multidimensional scaling: I. Theory and method*, Psychometrika, 17 (1952), pp. 401-419.

49. Z. Wang, S. Zheng, Y. Ye and S. Boyd, *Further relaxations of the semidefinite programming approach to sensor network localization*, SIAM J. Optim., 19 (2008), pp. 655-673.

50. F.C. Xing, *Investigation on solutions of cubic equations with one unknown*, J. Central Univ. Nat. (Natural Sci. Ed.), 12 (2003), pp. 207-218.

51. Z. Xu, X. Chang, F. Xu and H. Zhang, $L_{1/2}$ *regularization: a thresholding representation theory and a fast solver*, IEEE Trans. Neural Netw. Learn. Sys., 23 (2012), pp. 1013-1027.

52. G. Young and A.S. Householder, *Discussion of a set of points in terms of their mutual distances*, Psychometrika, 3 (1938), pp. 19-22.

53. L. Zhang, L. Liu, C. Gotsman and S.J. Gortler, *An as-rigid-as-possible approach to sensor network localization*, ACM Trans. Sen. Netw., 6 (2010), pp. 35:1-35:21.

54. L. Zhang, G. Wahba and M. Yuan, *Distance shrinkage and Euclidean embedding via regularized kernel estimation*, J. Royal Stat. Soc.: Series B, 78 (2016), pp. 849-867.

55. S.L. Zhou, N.H. Xiu and H.D. Qi, *A fast matrix majorization-projection method for constrained stress minimization in MDS*, available at https://www.researchgate.net/publication/319128036, 2017.